U.S. DEPARTMENT OF THE INTERIOR
U.S. GEOLOGICAL SURVEY

MAGMATIC CARBON DIOXIDE EMISSIONS AT MAMMOTH MOUNTAIN, CALIFORNIA

WATER-RESOURCES INVESTIGATIONS REPORT 98-4217

USGS
science for a changing world

Magmatic Carbon Dioxide Emissions at Mammoth Mountain, California

By CHRISTOPHER D. FARRAR, JOHN M. NEIL, *and* JAMES F. HOWLE

U.S. GEOLOGICAL SURVEY

Water-Resources Investigations Report 98–4217

7230-21

Sacramento, California
1999

U.S. DEPARTMENT OF THE INTERIOR
BRUCE BABBITT, Secretary

U.S. GEOLOGICAL SURVEY
Charles G. Groat, Director

For additional information write to:

District Chief
U.S. Geological Survey
Placer Hall, Suite 2012
6000 J Street
Sacramento, CA 95819-6129

Copies of this report can be purchased from:

U.S. Geological Survey
Information Services
Box 25286
Federal Center
Denver, CO 80225

CONTENTS

Abstract 1
Introduction 1
Background 1
Purpose and Scope 3
Acknowledgments 3
Location and Geologic History 3
Carbon Dioxide Emissions 4
Methods of Measurement and Investigation 5
Areas and Quantification of Emission 7
Trends 8
Potential Health Hazards 9
Source and Significance of Carbon Dioxide 11
Summary and Conclusions 12
References Cited 12

FIGURES

1,2. Maps showing:
1. Location of study area, Mammoth Mountain, California 2
2. Mammoth Mountain area: Selected topographic, geologic, and cultural features, and carbon dioxide sampling sites; and boundaries of tree-kill areas, sampling sites, carbon dioxide flux magnitudes, and carbon dioxide concentrations in soil ..... on plate 1
3. Schematic cross sections showing configuration of permanent soil-gas sampler installations, and monitoring-well site HSL-1 of ground-water monitoring well and soil-gas samplers in the unsaturated zone, Mammoth Mountain, California 6
4,5. Photographs showing:
4. Tree-kill areas near the base of the south face and the southwest side of Mammoth Mountain, and near the west shore of Horseshoe Lake, where carbon dioxide in the soil has killed nearly 100 percent of the trees in a 16-hectare area ..... on plate 1
5. Tree well containing air with high CO_2 concentration ..... on plate 1
6. Graph showing relation of oxygen and carbon dioxide derived from magmatic sources, Mammoth Mountain, California 10

TABLES

1. Soil gas carbon dioxide volumetric concentrations, Mammoth Mountain, California 14
2. Carbon dioxide flux (emission rate) at selected sites 23
3. Chemical analyses of water samples 30
4. Summary of carbon dioxide flux (emission rate) measurements 34

CONVERSION FACTORS, VERTICAL AND HORIZONTAL DATUMS

Multiply	By	To obtain
centimeter (cm)	0.3937	inch
cubic centimeter (cm^3)	0.06102	cubic inch
gram (g)	0.03527	ounce (avoirdupois)
gram per square meter per day [(g/m^2)]/d)	0.00345	ounce per square foot per day
millimeter (mm)	0.03937	inch
meter (m)	3.281	foot
kilometer (km)	0.6214	mile
square meter (m^2)	0.0002471	acre
hectare (ha)	2.471	acre
square kilometer (km^2)	247.1	acre
megagram per day (Mg/d)	1.102	ton per day

Temperature in degrees Celsius (°C) may be converted to degrees Fahrenheit (°F) as follows:

$$°F = (1.8 \times °C) + 32.$$

VERTICAL DATUM

Sea level: In this report, "sea level" refers to the National Geodetic Vertical Datum of 1929 (NGVD of 1929)—a geodetic datum derived from a general adjustment of the first-order level nets of both the United States and Canada, formerly called Sea Level Datum of 1929.

HORIZONTAL DATUM

In this report, the North American Datum of 1927 is used for Latitudes and Longitudes.

Magmatic Carbon Dioxide Emissions at Mammoth Mountain, California

By Christopher D. Farrar, John M. Neil, *and* James F. Howle

ABSTRACT

Carbon dioxide (CO_2) of magmatic origin is seeping out of the ground in unusual quantities at several locations around the flanks of Mammoth Mountain, a dormant volcano in Eastern California. The most recent volcanic activity on Mammoth Mountain was steam eruptions about 600 years ago, but seismic swarms and long-period earthquakes over the past decade are evidence of an active magmatic system at depth. The CO_2 emission probably began in 1990 but was not recognized until 1994. Seismic swarms and minor ground deformation during 1989, believed to be results of a shallow intrusion of magma beneath Mammoth Mountain, probably triggered the release of CO_2, which persists in 1998.

The CO_2 gas is at ambient temperatures and emanates diffusely from the soil surface rather than flowing from distinct vents. The CO_2 has collected in the soil by displacing air in the pore spaces and reaches concentrations of greater than 95 percent by volume in places. The total area affected by high CO_2 concentrations and high CO_2 flux from the soil surface was estimated at 60 hectares in 1997. Coniferous forest covering about 40 hectares has been killed by high CO_2 concentrations in the root zone.

In more than 300 soil-gas samples collected from depths of 0.5 to 2 m in 1995, CO_2 concentrations ranged from background levels (less than 1 percent) to greater than 95 percent by volume. At 250 locations, CO_2 flux was measured using a closed chamber in 1996; values, in grams per square meter per day, ranged from background (less than 25) to more than 30,000. On the basis of these data, the total emission of magmatic CO_2 in 1996 is estimated to be about 530 megagrams per day.

Concentrations of CO_2 exceeding Occupational Safety and Health Administration standards have been measured in pits dug in soil and snow, in poorly ventilated buildings, and in below-ground valve-boxes around Mammoth Mountain. CO_2 concentrations greater than 10 percent in poorly ventilated spaces are not uncommon on some parts of Mammoth Mountain. Humans and other animals exposed to CO_2 concentrations greater than 10 percent could lose consciousness and die rapidly. With knowledge of the problem and reasonable caution, however, the health hazard to humans can be avoided.

As noted earlier, the CO_2 emission is related to magmatic activity at depth, but at present (1998) it does not portend an imminent volcanic eruption.

INTRODUCTION

Background

Carbon dioxide gas is seeping out of the ground in unusually large amounts at several locations around the flanks of Mammoth Mountain (fig. 1, and fig. 2 on pl. 1). The emission of CO_2 at Mammoth Mountain is mostly diffuse from broad areas of the ground surface rather than from distinct vents, and because it is

generally colorless, odorless, and at ambient atmospheric temperatures, it may easily go undetected. At some locations, however, CO_2 has accumulated in the root zone of plants to concentrations high enough to kill forest vegetation. It was the unusual areas of tree kill noted by U.S. Forest Service personnel during the period 1990 to 1994 and a few reports of individuals who experienced symptoms of the early signs of asphyxia that prompted the U.S. Geological Survey (USGS) to begin an investigation that led to the identification of the anomalous CO_2 emissions described in this report. The source of the gas is either degassing magma that has intruded the shallow crust or degassing magma in combination with thermal decomposition of carbonate rocks. Diffuse emission of magmatic CO_2 from the land surface probably began in 1990 but was not recognized until 1994.

Mammoth Mountain is a dormant volcano. The emission of CO_2 from active or recently active volcanoes is not unusual (Gerlach, 1991). During the past two decades (1978–97), Mammoth Mountain and the adjacent Long Valley Caldera have had periods of moderate to intense geologic unrest that included periods of seismic swarm activity, earthquakes greater than magnitude 6, long-period earthquakes, and inflation of the land surface related to shallow intrusions of magma (Hill and others, 1985, 1990; Langbein, 1989; Langbein and others, 1995; and Pitt and Hill, 1994). The emission rate and composition of gas from Mammoth Mountain fumarole (MMF, fig. 2*A*) changed in response to seismicity beneath

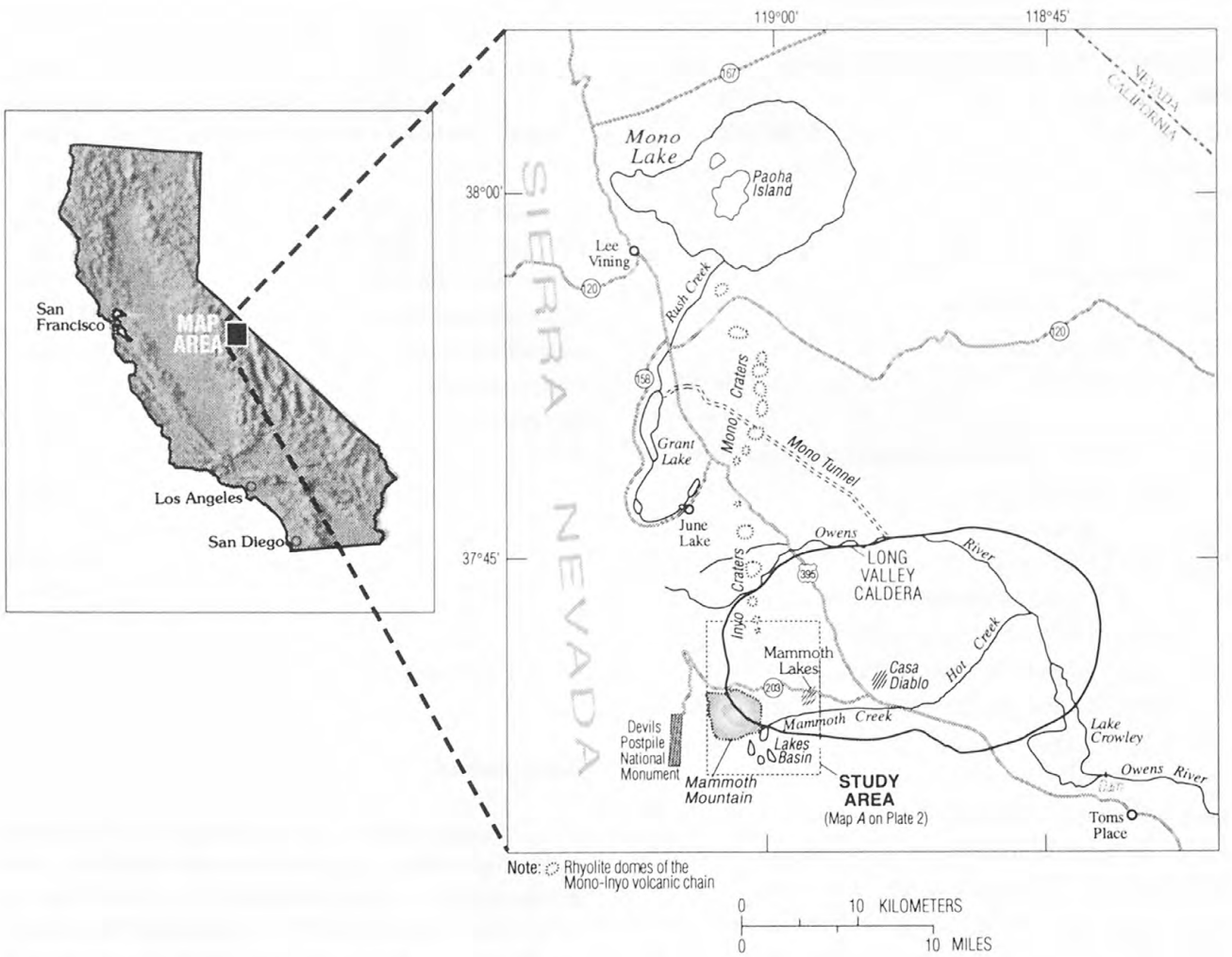

Figure 1. Location of study area, Mammoth Mountain, California.

Mammoth Mountain in 1989 (Sorey and others, 1993). The emission of CO_2 described in this report is the most recently recognized phenomenon related to the magmatic activity beneath the region (Farrar and others, 1995). None of these manifestations of geologic unrest necessarily portend an imminent volcanic eruption. Such cycles of unrest may wax and wane over hundreds or thousands of years without producing volcanic activity. Nevertheless, because of the relative strength and long duration of the unrest, a significant scientific effort to monitor and study the volcanic-hazard potential has been made by the USGS, other government agencies, and academic institutions. CO_2 emissions have now been added to the list of scientific parameters used to monitor volcanic hazards for the Mammoth Mountain-Long Valley Caldera region.

Purpose and Scope

Since 1980, the USGS has been studying the volcanic hazards in Long Valley Caldera and the Mono-Inyo Craters volcanic chain. This work includes monitoring seismic activity and other geophysical parameters, ground deformation, the hydrologic system, and gas emissions. The purpose of studying volcanic hazards is to provide information on the types of hazards that exist, to provide warnings prior to volcanic activity, to assist other agencies and the public by providing information on the present status of geologic unrest, and to broaden the understanding of volcanic systems and processes in general.

In 1994, as a part of the USGS volcanic hazards monitoring, CO_2 emissions were detected at Mammoth Mountain. Studies of the CO_2 emission have continued to date (1998) to help measure the levels of geologic unrest in the Mammoth Mountain area. The purpose of this report is to provide a description and maps of the magmatic CO_2 emission and brief discussions of the source, significance, and potential health hazards from the CO_2 gas. This report contains data from 1994 to 1996 for CO_2 concentrations in soil, CO_2 flux from the ground surface, and water chemistry for samples collected from selected sites around Mammoth Mountain. Visitors to the area can use this information to identify areas where CO_2 emissions are high and to gain a better understanding of why the emissions are occurring.

Acknowledgments

Fred Richter and Vernon McLean, U.S. Forest Service, provided key information relevant to this study and access to a Forest Service well and buildings. William Anderson, Mammoth Mountain Ski Corporation, provided information and access to wells at the ski area. William Evans, U.S. Geological Survey, provided chemical analyses for several gas samples included in this report. Elizabeth Colvard and Barry Kerr, U.S. Geological Survey, assisted extensively in soil gas sampling during the 1995 field season. Roy Bailey, U.S. Geological Survey, examined well cuttings and provided geologic interpretation.

LOCATION AND GEOLOGIC HISTORY

Mammoth Mountain is a large, geologically young volcano in the central Sierra Nevada and is located on the southwestern rim of the Long Valley Caldera at the southern end of the Mono-Inyo volcanic chain (fig. 1). Volcanic activity during the past few million years has had a tremendous effect on shaping the present-day landscape of this region of eastern California. The many volcanic mountains, domes, lava flows, phreatic explosion pits, areas of warm ground, thermal springs, and fumaroles all originate from frequent and varied types of volcanic eruptions or activity during recent geologic time. Long Valley Caldera is an elliptical, 20 km by 30 km, volcanic depression that formed 760,000 years ago as the result of a massive rhyolite ash-flow eruption. Later volcanic activity produced steep-sided domes, lava flows, and layers of volcanic ash within the caldera. Mammoth Mountain is composed of several dacitic and rhyolitic domes that were emplaced during the interval 200,000 to 50,000 years ago (Bailey, 1989). The summit of the broad-shouldered mountain is about 3,360 m above sea level and more than 1,200 m above the general level of the caldera floor.

The Mono-Inyo volcanic chain consists mainly of dozens of steep-sided rhyolite domes and a few phreatic explosion pits draped by a layer of pumice. This volcanic system, which extends 50 km from the north shore of Mono Lake southward to Red Cones, south of Mammoth Mountain, has been active frequently during the past 30,000 years (Bailey, 1989). The most recent activity near Mammoth Mountain produced several rhyolite domes (Inyo Craters in fig. 1)

and phreatic pits (locations shown in fig. 2*A* [see fig. 2 explanation]) less than 600 years ago (Miller, 1985), including several on the north flank of Mammoth Mountain. This activity was centered over a 10-km-long dike beneath the north flank of Mammoth Mountain that extends to beyond the northwestern boundary of the Long Valley Caldera (Fink, 1985). Much of the surface of the lower slopes of Mammoth Mountain is blanketed by light-colored pumice, as much as several meters thick, that was erupted during this most recent activity along the Mono-Inyo chain. At the north end of the chain, volcanic activity occurred on Paoha Island in Mono Lake as recently as 200 years ago. Although no volcanic activity is believed imminent (1998), there is no scientific basis to suggest that volcanic activity is finished in the Long Valley Caldera and the Mono-Inyo volcanic system.

The volcanic landforms have been modified by rotated fault-bounded blocks and erosional processes, including the action of glaciers. The final retreat of the glaciers occurred about 10,000 years ago in this part of the Sierra Nevada. The topography of the Lakes Basin, below the south flank of Mammoth Mountain, has been strongly affected by glacial scouring and by the deposition of moraines. These glacial processes produced numerous depressions, several of which now are filled by small lakes. When the glaciers retreated, a veneer of glacial outwash was deposited that now partially blankets the underlying granitic and volcanic rocks.

Granitic and metamorphic rocks that make up the core of the Sierra Nevada crop out around the periphery of Mammoth Mountain on the south, west, and north sides. The metamorphic rocks are present as discontinuous masses enclosed by the more extensive granitic rocks that also underlie the volcanic pile that composes Mammoth Mountain. Metamorphic rocks might also be present beneath the mountain.

CARBON DIOXIDE EMISSIONS

Several areas of high CO_2 flux and soil-gas concentrations have been identified on the north, west, and south flanks of Mammoth Mountain, mostly at altitudes above 2,700 m (fig. 2*A* and tables 1 and 2). In this report these areas are referred to as "CO_2 anomalies" or "anomalous areas" because either the soil-gas concentration or the flux is elevated significantly above typical background values measured well outside the anomalies. The emission of CO_2 from soils is a natural component of biologic activity. In forest soils of the eastern Sierra, background CO_2 emissions are variable but generally are less than 25 $(g/m^2)/d$. In the CO_2 anomalies, fluxes greater than 30,000 $(g/m^2)/d$ have been measured and generally exceed 100 $(g/m^2)/d$ (table 2). Each of the main anomalous areas has been given a name based on a local geographic feature for easy reference. These names are used in the maps, tables, and graphs. Maps at an enlarged scale of 1:6,000 show more detailed views of each of the main areas (figs. 2*B–G*).

Soil gas in the anomaly areas is largely an enriched mixture of CO_2 in air. In the table that follows, chemical analyses of soil gas from two of the anomalous areas are compared with analyses of soil gas from a control site (outside the anomalous area) and an atmospheric sample. These soil-gas samples were collected from a depth of 1 m. The two samples with elevated CO_2 concentrations contain proportionately less oxygen, nitrogen, and argon than do the samples from the control site and the atmosphere.

Chemical analyses of soil-gas and atmospheric samples

(Analyses by W.C. Evans, USGS, Menlo Park, California. Values expressed in volume percent)

	Soil gas			
	Chair 12 anomalous area	Horseshoe Lake anomalous area	Control Site (live trees)	Local Atmosphere
Carbon dioxide	96.526	47.831	0.498	0.037
Nitrogen	2.913	41.103	78.106	78.100
Oxygen	.531	10.588	20.444	20.946
Argon	.028	.480	.952	.934
Helium	.0013	.0008	.0005	.0005
Hydrogen sulfide	<.0005	<.0005	<.0005	<.0005

In the anomalous areas, CO_2 concentrations range from greater than 1 to greater than 95 percent by volume. Helium is the only other gas found to occur in unusually high concentrations relative to air; but in terms of volume percent, it is a very minor constituent. Excesses of sulfur gases compared to air are conspicuously missing from the soil gas even though a magmatic origin for the CO_2 is indicated.

Green plants take in CO_2 through their leaves produce energy to grow by photosynthesis and respire oxygen to the atmosphere. Slightly elevated CO_2 levels in the atmosphere around plants has been found to accelerate growth and often is beneficial to the plants (Heath and others, 1993). However, elevated concentrations of CO_2 in the root zone can be toxic to plants (Qi and others, 1994). Normally, the air in soil contains less than a few percent CO_2. When the level exceeds 10 to 20 percent, root development is inhibited—hence water and nutrient uptake are decreased. Soil pH also may be affected by uncommonly high concentrations of CO_2. The concentration of CO_2 in the root zone that causes vegetation to die depends on many factors, including the length of exposure, presence or absence of other gases, soil moisture conditions, amounts of nutrients, and the species of plants. At Mammoth Mountain, the forest vegetation usually begins to show signs of stress when soil-gas concentrations of CO_2 are 20 percent or greater.

There are two measures by which CO_2 can be quantified: concentration and mass flow rate or flux. In this report, concentration refers to volumetric concentration in parts per million or percent at a depth of 0.5 m, unless otherwise stated. Flux is a measure of the rate of CO_2 moving across a surface or boundary and is expressed as units of mass (grams [g] or megagrams [Mg]) per time (hours or days) from a specified area (square meters or hectares [ha]). Both types of measurements have been made on Mammoth Mountain. The relation between concentration and flux is not necessarily direct. A volume of soil may contain a high concentration of CO_2 but have a low flux at the surface; conversely, a volume of soil with relatively low CO_2 concentration can produce a relatively high flux. The relation varies because the flux is dependent on both the concentration and the rate of movement. The rate of movement is controlled, in part, by the permeability of the soil. Gas-flow rates are lower from areas underlain by soils with low gas permeability than from areas underlain by soils with high permeability when other factors are equal.

Methods of Measurement and Investigation

Surveys for locating CO_2 anomalies have been done in the locations shown in figure 2. Surveys included transects along which soil-gas samples were extracted from depths of 0.5 to 2 m and analyzed for CO_2 concentration and grids of sites where emission rates were measured. The surveys initially focused on any areas where the forest appeared unhealthy or where a large percentage of the trees were dead. Aerial photographs and multispectral images collected from low-altitude fixed-wing aircraft were used to aid in mapping and identifying areas of dead and dying forest. High concentrations of CO_2 were not found in all the tree-kill areas, and some of the tree-kills were clearly caused by insect infestations or fire. Other transect lines were run along access roads, along which samples were collected at roughly uniform spacing. These lines were designed to provide a survey not biased by the visual appearance of vegetation.

The CO_2 concentrations were determined in the field using a gas chromatograph stationed at a central location. Samples of soil gas were collected in 5-cm^3 glass syringes and analyzed within a few hours of collection. The soil-gas sampler consisted of a 1- to 2-m long, 1-cm inside diameter (I.D.) steel pipe, pointed at the bottom end and containing 3-mm perforations in the bottom 8 cm of pipe (as shown in the schematic diagram, fig. 3*A*). A 2-mm I.D. Teflon tube, isolated from the rest of the pipe by a rubber packer extended from the top end of the steel pipe to the perforated section. Sampling syringes with valves were fitted directly on the upper end of the Teflon tube. Samples were collected after the steel pipe was driven to the specified depth and the stale gas was purged from the Teflon tubing by removing at least two volumes of gas. At 14 sites, samplers similar to those described above were left permanently installed in the ground (locations are shown in figs. 2*A*-*G*). Each of these sites had three samplers set to depths of 0.5, 1.0, and 2.0 m (fig. 3*A*). Samples collected at different times from the permanent sampler locations were analyzed to identify concentration variations at shallow depths and temporal trends.

The CO_2 flux values were determined using closed-dynamic-accumulation chambers in which the

rate of change in concentration was measured (Rolston, 1986; Norman and others, 1997). The chambers ranged in volume from 10 to 14 liters and had diameters of 22 to 38 cm. In 1995, concentrations were measured with a gas chromatograph for samples collected in syringes filled from a port on the chamber at intervals from 1 to 5 minutes. In 1996, concentrations were measured using an infrared gas analyzer that received gas pumped in a continuous loop from and back into the chamber. Readings from this system were recorded at frequencies of 2 to 30 seconds for durations of 30 seconds to 5 minutes. The flux was calculated from $\Delta c/\Delta t$ (change in concentration for a time interval) using a best-fit linear equation.

Two monitoring wells were drilled in areas of CO_2 anomalies to learn more about variations in concentrations in the unsaturated zone and the chemistry and isotopic composition of ground water. Well HSL-1 (fig. 2*E*), at Horseshoe Lake, is 98 m deep and well CH-11A (fig. 2*F*), on the north side of the mountain, is 61 m deep. The method of completion of the wells was similar; construction details for well HSL-1 are shown in figure 3b. Four 3-mm I.D. polyethylene tubes were installed over a range of depths from 5 m to near the water table (generally less than 45 m) for collecting soil-gas samples. Each well also has a 5-cm-diameter polyvinyl chloride pipe extending to the full depth of the well, with

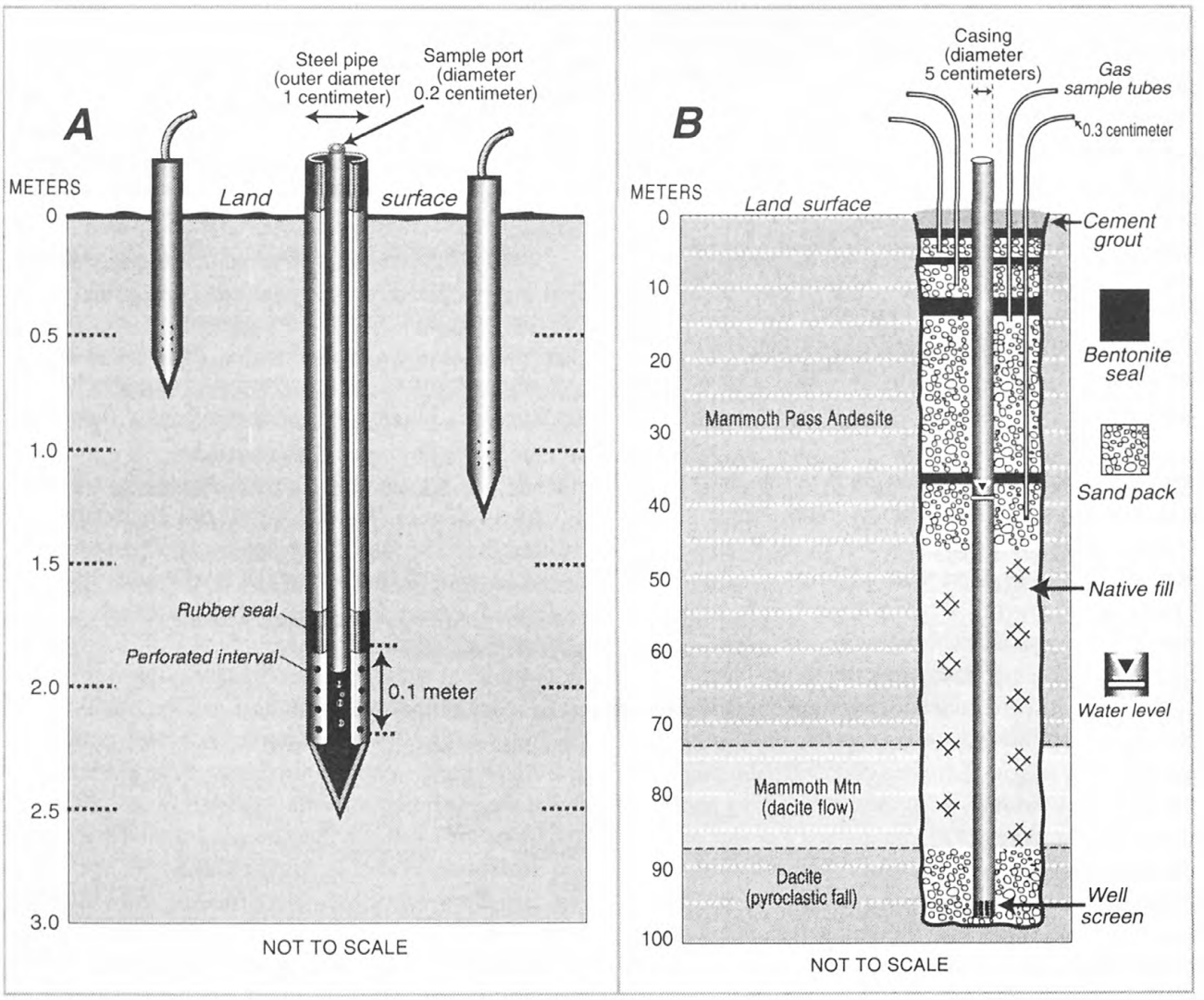

Figure 3. Configuration of *A*, permanent soil-gas sampler installations, and *B*, monitoring-well site HSL-1 of ground-water monitoring well and soil-gas samplers in the unsaturated zone, Mammoth Mountain, California.

perforations in the bottom 3 m, for collecting water samples and measuring water levels.

Areas and Quantification of Emission

Most of the known CO_2 anomalies are below tree line (about 3,100 m above sea level) and have been identified because the tree-kill (high level of forest mortality) has provided a dramatic visual means for locating them (figs. 4*A-C*). As noted earlier, normal soils of the eastern Sierra Nevada have relatively low levels of biologic activity and contain 1 percent or less CO_2 by volume in the soil pores. In the anomalous areas, CO_2 concentrations greater than 95 percent have been measured. The association between areas with high concentrations of soil-gas CO_2 and areas of tree-kill with nearly 100-percent mortality is clear from the relation of CO_2 concentration and the health of trees along transect lines. However, it is important to emphasize that not all patches or areas of dead or dying conifers on Mammoth Mountain are the result of high concentrations of CO_2 in the soil; many trees have died from more routine causes, such as insect damage, drought, or fire.

Although the anomalous areas contain volumes of soil with extraordinarily high concentrations of CO_2 and emission rates thousands of times greater than in normal areas, the concentration of CO_2 in the atmosphere 1 to 2 m above land surface over these areas is generally no greater than two or three times the world mean concentration (about 360 parts per million [ppm]). Apparently, the CO_2 emitted from the soil rapidly dissipates by convection and diffusion into the atmosphere.

The anomalous areas identified so far are all west of the developed part of the Town of Mammoth Lakes (fig. 2). The Horseshoe Lake area is the most notable CO_2 anomaly because of its large area (12 ha or about 30 acres) and nearly complete mortality of the forest within the area (figs. 4*B* and 4*C*). The Horseshoe Lake area is a popular and easily accessible campground and day-use area for local residents and tourists. Some of the other anomalous areas are less accessible and the level of forest mortality is less complete. The anomalous areas above tree line are more difficult to find because of the lack of visually discernible characteristics. Some of the known anomalies are near to faults mapped by Bailey (1989). Reconnaissance of areas adjacent to faults above tree line has identified a few areas of high CO_2 concentrations and emissions. But the accounting of all CO_2 anomalies above and below tree line is still not comprehensive. As of September 1997 about 40 ha (approximately 100 acres) of forest had been killed by high concentrations of CO_2 in the root zone. The total surface area of known CO_2 anomalies, including tree-kill areas, enclaves of bare soil, areas of live forest, and areas above tree line was estimated to be about 60 ha (approximately 150 acres).

The change in the concentrations of CO_2 in the soil from land surface to a depth of 2 m has been measured at 14 sites on Mammoth Mountain. Generally, the CO_2 concentration increases (positive gradient) with depth in the upper 2 m. But at some locations, reverse gradients or no discernible gradient has been found. These abnormal gradients are most likely caused by heterogeneities of soil-moisture distribution or soil texture and complexities of convective mixing. At well HSL-1, gas-sampling ports have been placed at four depths between 5 and 42 m (42 m is near the water table). The lack of a discernible CO_2 concentration gradient over the full thickness of the unsaturated zone at this site suggests either that the CO_2 is flowing laterally from a source area topographically upgradient from HSL-1 or that the CO_2 flux is driven more by a pressure gradient than by chemical diffusion.

Seasonal variations in CO_2 concentrations at selected locations and depths in the soil have been measured. CO_2 concentrations in samples collected from three permanent soil-gas samplers in the Horseshoe Lake area are given in the table that follows.

Carbon dioxide concentration in soil gas

[Sample depth 1 meter; values expressed in volume percent]

Site	Setting	December 1, 1995	March 20, 1996	April 19, 1996	June 19, 1996	July 16, 1996
HSL-PS1	Edge of tree-kill	3.5	9.0	10.5	3.3	2.7
HSL-PS3	Edge of tree-kill	6.5	51.1	57.6	10.5	8.3
HSL-PS4	Central part of tree-kill	71.8	72.0	—	70.9	71.5

Sampler sites HSL-PS1 and HSL-PS3 are located along the edge of the Horseshoe Lake tree-kill area, and both show a strong seasonal variation in CO_2 at a depth of 1 m. Site HSL-PS4 is located in the central part of the Horseshoe Lake tree-kill area, and the CO_2 concentration shows little seasonal variation.

The variation in CO_2 concentration is primarily in response to levels of snow cover and soil moisture (McGee and Gerlach, 1998). Immediately following a snowfall, the concentration rises until a new equilibrium emission rate is established. In addition, depending on the water content and density of a snow pack, the emission of CO_2 from the surface can be retarded, causing the concentration in the soil to increase further. The winters of 1995 and 1996 produced above-average snow packs on Mammoth Mountain. Deep accumulations of snow and ice layers tend to inhibit gas emission from the surface and cause the area of CO_2 anomaly to increase. This process partly explains the increase in CO_2 measured at HSL-PS1 and HSL-PS3, where the concentrations were highest during March and April 1996 when snow depth was at a maximum. The area of high soil-gas CO_2 concentration also may have increased temporarily during the winters of 1995 and 1996, causing an enlargement of the areas of tree-kill in comparison with the summer of 1994. The lack of seasonal variation at HSL-PS4 suggests that this site may be closer to the main CO_2 upflow area.

Liquid water entering the soil also affects the CO_2 concentration and the CO_2 emission rate. When water from rain or melting snow infiltrates below the land surface, soil pores become water saturated, inhibiting the movement of soil gas. The infiltrated water also has the capacity to dissolve CO_2 and carry it away in the ground-water flow system, thus decreasing the total mass of gas emitted at the land surface. In contact with water, CO_2 gas dissolves until saturation is reached. The saturation concentration is partly dependent on the temperature and pressure. Some of the dissolved gas reacts with water molecules to form carbonic acid (H_2CO_3); this is a weak acid, some of which ionizes to form hydrogen and bicarbonate ions (Stumm and Morgan, 1996). Therefore, determining pH and the concentrations of bicarbonate and other dissolved inorganic carbon species in water samples from near the CO_2 anomalies can provide clues to the distribution and quantity of magmatic CO_2 emission. Water samples from five wells, one spring, and Horseshoe Lake were analyzed (table 3). These analyses can be used as a baseline for comparison with future analyses; changes in chemical composition might be an indication of changes in CO_2 emission rate. Horseshoe Lake was chosen for sampling to test for the possible buildup of CO_2 in the lake water. In some volcanic areas, the sudden turnover of lakes has released hazardous amounts of CO_2 and caused the loss of human lives (Tuttle and others, 1987; Baxter and Kapila, 1989). However, no large accumulation of CO_2 was detected in Horseshoe Lake—probably because the lake turns over annually and also loses a large volume of water through seepage and(or) flow to fissures in the lake bottom.

Trends

Long-term trends in the total area-wide emission rate of CO_2 are more difficult to establish with confidence than are seasonal trends at specific sites because of the high variance in the emission rates measured between sites as close as a few meters apart. Also, emission rates measured months apart might differ because of variations in near-surface atmospheric conditions (for example, air pressure and winds) and soil moisture rather than changes in the CO_2 source.

On the basis of detailed land-based mapping, the tree-kill areas at Horseshoe Lake and Chair 12 did not change significantly between August 1995 and August 1996. This is an indication that the surface area of CO_2 emission did not increase in these two areas. Detailed mapping of tree-kill was not done in the other CO_2 anomalous areas because some are above tree line and others have more poorly defined boundaries. On the basis of field observations, however, the area of dying trees probably did increase during this period on the north side of Mammoth Mountain near the ski area lodge.

The total mass of magmatic CO_2 emitted from Mammoth Mountain is estimated to be about 530 Mg/d, on the basis of measurements made during August and September 1996 (table 4). This estimate, although somewhat greater than the rate of 400 Mg/d estimated by Rahn and others (1996), is less than the rate of 1,200 Mg/d estimated by Farrar and others (1995). The difference most likely is due to the larger number of measurements used to calculate the 1996 estimate (this study) rather than a change in the total mass emitted.

Gerlach and others (1998) have measured large variations in the total CO_2 emission from the Horseshoe Lake CO_2 anomaly between 1995 and 1997. Between August 30, 1995, and September 12, 1997, their measurements show a decline from 350 to 130 Mg/d, which they attribute to a long-term decline. But 11 days later, on September 23, 1997, they measured 220 Mg/d; they attribute this large rapid change to a degassing event caused by dilation of fractures in response to local crustal deformation.

POTENTIAL HEALTH HAZARDS

Humans and other animals take in oxygen and expel CO_2 during respiration. CO_2 is normally present in the atmosphere at concentrations of about 360 to 370 ppm. Exposure to CO_2 concentrations greater than 5,000 ppm can be a health hazard. The Occupational Safety and Health Administration (OSHA) and the National Institute of Health and Safety have issued guidelines for safe levels of exposure to CO_2 (National Institute for Occupational Safety and Health, 1979). Two factors contribute to the health hazard in environments with high levels of CO_2 (Stupfel and LeGuern, 1989). First, at concentrations greater than 10 percent [10,000 parts per million (ppm)], CO_2 is toxic, causing physiologic effects that can lead to respiratory and cardiac arrest. Second, large amounts of CO_2 can displace air and reduce the amount of available oxygen.

The risk of asphyxiation from high concentrations of CO_2 around Mammoth Mountain is a serious health hazard but one that generally can be avoided easily. Although the CO_2 concentrations in the shallow soil is very high in places, the CO_2 is emitted from the surface at rates sufficiently low to allow ordinary atmospheric circulation to dilute the gas to levels well below any health advisory at a short distance above ground. Known areas of high concentrations and emission rates are shown in figure 2 (see pl. 1); however, other parts of the mountain, not yet investigated, could also contain high-emission areas. Carbon dioxide gas is not visible to humans and generally cannot be detected by taste or smell below concentrations of 10 to 20 percent. This lack of easy detection means that avoidance of any enclosed spaces without ventilation systems and any natural or man-made depressions in the soil or snow (fig. 5 [on pl. 1]) on Mammoth Mountain is the best means of preventing exposure to unhealthy concentrations of CO_2.

In areas of high CO_2 emission, specific activities or conditions that could lead to exposure to unhealthy CO_2 concentrations include, but are not limited to: occupying a tent, digging holes in soil or snow, occupying a snow cave, entering a tree-well (fig. 5), entering the space between the snow pack and a building, lying on or near the ground surface, or entering a poorly ventilated building or below-ground vault.

Miscellaneous measurements made between 1994 and 1997 (see table that follows) have found high CO_2 concentrations in poorly ventilated spaces at several locations around Mammoth Mountain.

Persons entering areas of high CO_2 concentration or emission can use the standards set by OSHA and the National Institute for Occupational Safety and Health (NIOSH) as a measure of potential over-exposure. The permissible exposure limits for

General levels of carbon dioxide concentration in poorly ventilated spaces around Mammoth Mountain

Site description	CO_2 concentration (volume-percent)
Snow pits, 1 or more meters deep	As great as 70
Cavities in snow around restrooms at Horseshoe Lake	As great as 40
Tree-wells around dead trees at Horseshoe Lake	As great as 60
Vault–below ground, water-valve boxes	Greater than 80
Snow cabin, near Horseshoe Lake	As great as 25
Restroom, closed about 7 months for winter	Greater than 2

employees in workspaces are specified by OSHA as 5,000 ppm (0.5 percent) CO_2 for the time-weighted average during an 8-hour period and 15,000 ppm (1.5 percent) CO_2 for a 15-minute exposure period. A ceiling exposure limit of 30,000 ppm (3 percent), not to be exceeded for any length of time, has been recommended by NIOSH. According to Budavari and others (1989) humans can not breathe air containing more than 10 percent CO_2 without losing consciousness.

Signs of overexposure to CO_2 by inhalation include rapid breathing, rapid heart rate, headache, sweating, shortness of breath, dizziness, mental depression, visual disturbances, shaking, unconsciousness, and death.

The recommended emergency first aid for individuals exposed to high concentrations of CO_2 is to move the person to fresh air immediately; perform rescue breathing (formerly referred to as artificial respiration) or cardiopulmonary resuscitation (CPR) if needed; keep patient warm and at rest, and get medical attention as soon as possible (Joseph, 1985).

In areas around Mammoth Mountain where CO_2 concentrations are abnormally high, oxygen is depleted. The depletion of oxygen in volume-percent is approximately at a ratio of 1 to 5 relative to the CO_2 concentration (fig. 6). For example, as the CO2 concentration increases near zero to 25 percent (see fig. 6), the concentration of oxygen decreases from about 21 percent to about 16 percent by volume. This is because in areas of high CO_2 concentration around Mammoth Mountain, normal air is depleted in an amount approximately equal to the CO_2 concentration, and oxygen makes up about one-fifth of air by volume. OSHA designates any atmosphere as oxygen deficient if oxygen is present at less than 19.5 percent by volume. According to this standard, air containing CO_2 in excess of approximately 7 percent by volume is oxygen deficient, in addition to containing a dangerous level of CO_2.

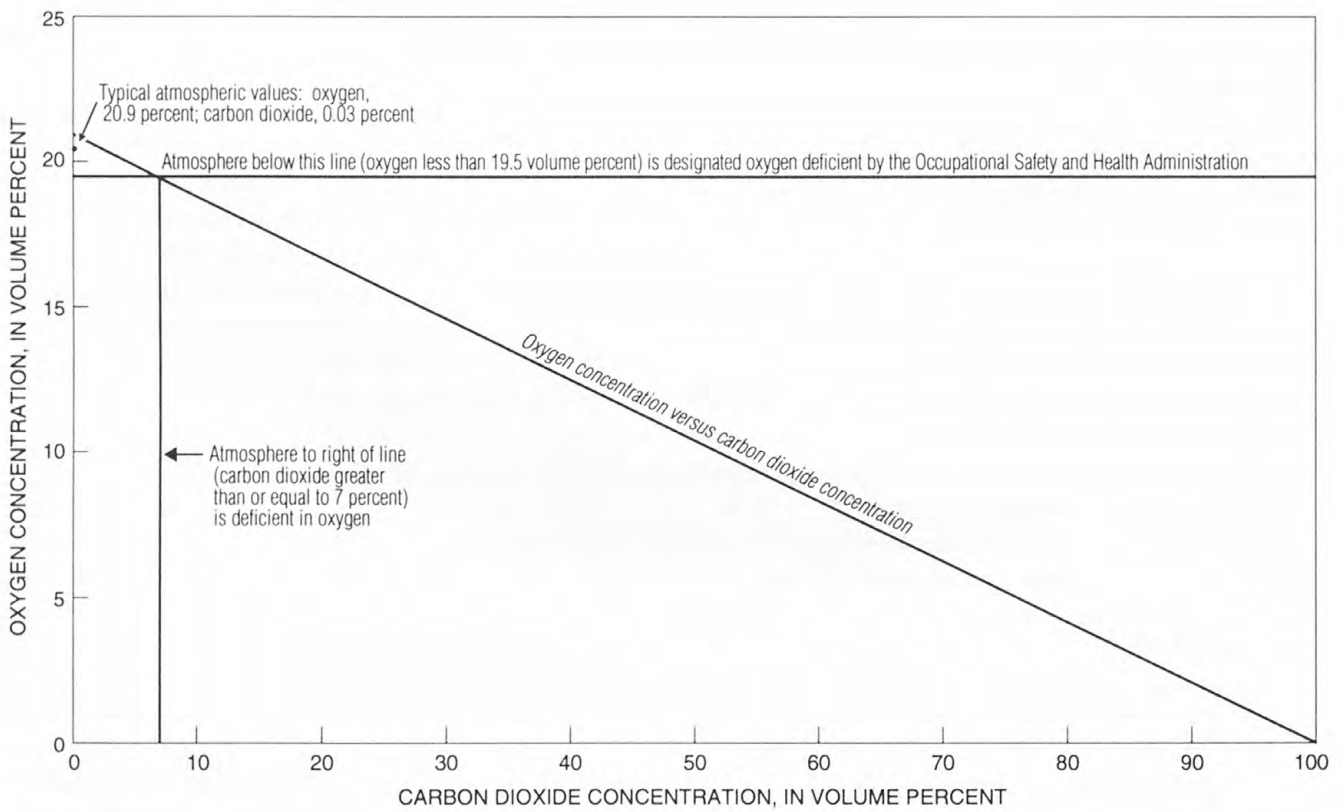

Figure 6. Relation of oxygen and carbon dioxide derived from magmatic sources, Mammoth Mountain, California.

SOURCE AND SIGNIFICANCE OF CARBON DIOXIDE

Several lines of evidence indicate that the CO_2 emission from Mammoth Mountain is of magmatic origin. The estimated 530 Mg/d is much larger than can be expected from biologic activity. Isotopic analyses of carbon and helium in the soil gas (Farrar and others, 1995; Sorey and others, 1993; Sorey and others, 1998) show that the source is deep-seated (either from the mantle or deep crust). The timing of the release of the gas from the land surface is also consistent with a magmatic origin. In a 6-month period during 1989, activity in a region beneath Mammoth Mountain produced a large number of small-magnitude earthquakes and a small amount of deformation of the mountain surface. The cause of this activity was a small intrusion of magma into the shallow crust (discussed later) beneath Mammoth Mountain (Hill and others, 1990; Hill, 1996). Occassional long-period earthquakes at depths of 15 to 20 km have been recorded in the vicinity of Mammoth Mountain since 1989 (Pitt and Hill, 1994) and are further evidence of magma moving from the mantle into the crust beneath the Mammoth region. Although no CO_2 measurements were made until 1994, the onset of tree-kills, later recognized as caused by CO_2, were first noted in 1990. A U.S. Forest Service ranger reported symptoms of asphyxia when he entered a snow-covered cabin near Horseshoe Lake in March 1990 (Fred Richter, oral commun., 1994). The asphyxia symptoms most likely were caused by a buildup of CO_2 in the cabin, which lacked proper ventilation. Thus, it can be concluded that large amounts of CO_2 were accumulating in and emitting from the soil within 6 months after the 1989 seismic-swarm and magmatic intrusion.

Although compelling evidence for a magmatic origin for the CO_2 exists, the mechanism of CO_2 accumulation and release is less certain. The gas could be released directly from small magma bodies intruded since 1989, or it could be released through fractures in the seal over a gas-rich reservoir that could have accumulated CO_2 from many intrusions over a period of hundreds or thousands of years. Additional CO_2 could be generated from thermal decomposition of carbonate rocks in the subsurface, but this still requires magma for a heat source. The surface exposures of metasedimentary rocks that contain carbonate minerals near Mammoth Mountain are shown in figure 2*A*. The subsurface distribution is not known; however, the proximity of surface exposures suggests that the same rocks may be present beneath the mountain and potentially could contribute to the CO_2 emission.

Seismic data from earthquakes near Mammoth Mountain suggest that the source magma for the CO_2 is from 2 to 18 km beneath the surface and most likely is greater than 4 km deep (Julian and others, 1998). Most of the known CO_2 anomalies are on or near mapped faults (fig. 2*A*). The CO_2 travels from the source to the land surface through open fractures in the crystalline rocks and through intergranular pore spaces in the overlying sediment and soil. The open fractures are related to faults and joint systems produced by regional and local deformation. Pressure gradient is probably the main driving force that produces flow of CO_2 from the source to the land surface, but the gas also moves by diffusion. Density is an additional factor that controls the movement and distribution of CO_2 gas, especially near the land surface. Carbon dioxide can displace air because it is approximately 1.53 times the density of air. This process accounts for CO_2 accumulation in surface depressions and below-ground enclosed spaces. The same process causes CO_2 to flow through intergranular pore spaces down topographic gradients.

Ground water is present at depths of 15 to 45 m at locations where wells have been drilled on Mammoth Mountain. Ground water occurs in a number of shallow perched aquifers and in one or more deeper flow systems in fractured rocks. Because ground water is widely distributed beneath Mammoth Mountain and the same fractures that allow for transport of gas are saturated with ground water, CO_2 must pass through ground water along its path from source area to the land surface. The occurrence of carbonated springs and wells on Mammoth Mountain support the notion of gas transport through ground water. Gas transport through ground water could also explain the lack of sulfur gases in the CO_2 emission areas because sulfur dioxide and hydrogen sulfide are more soluble than CO_2 in water. It is possible that the dissolved sulfur gases are being transported away from the CO_2 emission areas in the ground-water flow system.

The anomalous emission of CO_2 corroborates the seismic and geodetic evidence that magma has recently intruded into the shallow crust beneath Mammoth Mountain. The amount and rate of accumulation of magma are two factors that control the onset of eruptive activity in a volcanic system. Future

changes in the rate of CO_2 emission may occur in response to new intrusions of magma emplaced beneath Mammoth Mountain. The possibility of CO_2 produced from thermal decomposition of carbonate rocks heated by magma complicates the relation between volume of magma and rate of CO_2 emission.

SUMMARY AND CONCLUSIONS

The CO_2 emission described in this report is one of the surface expressions of ongoing volcanic processes in a dormant but restless volcanic system. The ultimate source of the CO_2 is degassing magma in the crust beneath the Mammoth Mountain area. The emission does not presage an imminent eruption but has produced damaging effects to vegetation on at least 40 ha of coniferous forest, has caused the closing of a U.S. Forest Service campground, and poses a significant but avoidable human health risk on some parts of Mammoth Mountain. Identifying all the areas of magmatic gas emission, quantifying the total mass, and measuring changes in the emission rate will be useful, along with seismic and deformation monitoring, for assessing the potential for future volcanic activity at Mammoth Mountain and the health risks from CO_2.

Most of the known CO_2 anomalies occur in six areas below tree line (3,100 m above sea level) around the south, west, and north sides of Mammoth Mountain. Prominent tree-kills are associated with each of the areas. All the areas are west of the developed part of the town of Mammoth Lakes. The CO_2 concentration in the soil in anomalous areas is as high as 96 percent by volume. The CO_2 flux in several locations is greater than 1,000 $(g/m^2)/d$. On the basis of measurements, the total emission of CO_2 in 1996 is estimated to be 530 Mg/d.

The concentration of CO_2 in soil varies seasonally in relation to accumulated snow because the snow inhibits the flow of gas to the surface; CO_2 also collects in the snow pack in the pores between snow and ice crystals. Rapid changes in the total CO_2 flux from the Horseshoe Lake area have been documented by Gerlach and others (1998). Such changes might be caused by local seismicity that causes fractures to open.

REFERENCES CITED

Bailey, R.A., 1989, Geologic map of Long Valley Caldera, Mono-Inyo Craters volcanic chain, and vicinity, eastern California: U.S. Geological Survey Miscellaneous Investigations Series Map I-1933, 2 sheets.

Baxter, P.J. and Kapila, Mukesh, 1989, Acute health impact of the gas release at Lake Nyos, Cameroon, 1986: Journal of Volcanology and Geothermal Research, v. 39, p. 265-275.

Budavari, S., Dale, M., O'Neil, J., and Smith A., eds., 1989, Merck Index—Encyclopedia of chemicals, drugs, and biologicals (11th ed.): Rahway, NJ, Merck and Company [variously paged].

Farrar, C.D., Sorey, M.L., Evans W.C., Howle, J.F., Kerr, B.D., Kennedy, B.M., King, C.-Y, and Southon, J.R., 1995, Forest-killing diffuse CO_2 emission at Mammoth Mountain as a sign of magmatic unrest: Nature v. 376, p. 675-678.

Fink, J.H., 1985, Geometry of silicic dikes beneath the Inyo Domes, California: Journal of Geophysical Research, v. 90, no. B13, p. 11,127-11,133.

Gerlach, T.M., 1991, Present-day CO_2 emissions from volcanos: Eos, Transactions, American Geophysical Union, v. 72, no. 23, p. 249, 254-255.

Gerlach, T.M., Doukas, M.P., McGee, K.A., and Kessler, R., 1998, Three-year decline of magmatic CO_2 emissions from soils of a Mammoth Mountain tree kill: Horseshoe Lake, CA, 1995-1997: Geophysical Research Letters, v. 25, p. 1947-1950.

Heath, L.S., Kauppi, P.E., Burschel, Peter, Gregor, H.D, Guderian, Robert, Kohlmaier, G.H., Lorenz, Suzanne, Overkieck, Dieter, Scholz, Florian, Thomasius, Harald, and Weber, Michael, 1993, Contribution of temperate forests to the world's carbon budget: Water, Air, and Soil Polution, v. 70, p. 55-69.

Hill, D.P., 1996, Earthquakes and carbon dioxide beneath Mammoth Mountain, California: Seismological Research Letters, v. 67, no. 1, p. 8-15.

Hill, D.P., Bailey, R.A., and Ryall, A.S., 1985, Active tectonic and magmatic processes beneath Long Valley Caldera, eastern California: An overview: Journal of Geophysical Research v. 90, no. B13, p. 11,111-11,120.

Hill, D.P., Ellsworth, W. L., Johnston, M.J.S., Langbein, J.O., Oppenheimer, D.H., Pitt, A.M., Reasenberg, P.A., Sorey, M.L., and McNutt, S.R., 1990, The 1989 earthquake swarm beneath Mammoth Mountain, California: An initial look at the 4 May through 30 September activity: Bulletin of the Seismological Society of America v. 80, no. 2 p. 325-339.

Joseph, E.Z., ed., 1985, Chemical safety data guide: Bureau of National Affairs, 927 p.

Julian, B.R., Pitt, A.M., and Foulger, G.R., 1998, Seismic image of a CO_2 reservoir beneath a seismically active volcano: Geophysical Journal International, 133, p. F7-F10.

Langbein, John, 1989, Deformation of the Long Valley Caldera, eastern California from mid-1983 to mid-1988: Measurements using a two-color geodimeter: Journal of Geophysical Research, v. 94, no. B4, p. 3833-3849.

Langbein, John, Dzurisin, Daniel, Marshall, Grant, Stein, Ross, and Rundle, John, 1995, Shallow and peripheral volcanic sources of inflation revealed by modeling two-color geodimeter and leveling data from Long Valley caldera, California, 1988-1992: Journal of Geophysical Research v. 100, no. B7, p. 12,487-12,495.

McGee, K.A. and Gerlach, T.M., 1998, Annual cycle of Magmatic CO_2 at Mammoth Mountain, California: Implications for soil acidification: Geology, v. 26, no. 5, p. 463-466.

Miller, C.D., 1985, Holocene eruptions at the Inyo volcanic chain, California: implications for possible eruptions in Long Valley: Geology v. 13, p. 14-17.

National Institute for Occupational Safety and Health, 1979, Recommended standard for occupational exposure to carbon dioxide: U.S. Department of Health, Education, and Welfare, 6 p.

Norman, J.M., Kucharik, C.J., Gower, S.T., Baldocchi, D.D., Crill, P.M., Rayment, M., Savage, K., and Striegl, R.G., 1997, A comparison of six methods for measuring soil-surface carbon dioxide fluxes: Journal of Geophysical Research, v. 102, no. D24, p. 28,771-28,777.

Pitt, A.M. and Hill, D.P., 1994, Long-period earthquakes in the Long Valley caldera region, eastern California: Geophysical Research Letters, v. 21, no. 16, p. 1679-1682.

Qi, J., Marshall, J.D., and Matson, K.G., 1994, High soil carbon dioxide concentrations inhibit root respiration of Douglas Fir: New Phytology, v. 128, p. 435-441.

Rahn, T.A., Fessenden, J.E., and Wahlen, M., 1996, Flux chamber measurements of anomalous CO_2 emission from the flanks of Mammoth Mountain, California: Geophysical Research Letters, v. 23, p. 1861-1864.

Rolston, D.E., 1986, Methods of soil analysis part 1, *in* Klute, Arnold, ed., Physical and mineralogical methods (2d ed.), Madison, WI, American Society of Agronomy and Soil Science Society of America, p. 1103-1119.

Sorey, M.L., Kennedy, B.M., Evans, W.C., Farrar, C.D., and Suemnicht, G.A., 1993, Helium isotope and gas discharge variations associated with crustal unrest in Long Valley Caldera, California, 1989-1992: Journal of Geophysical Research, v. 98, no. B9, p. 15,871-15,889.

Sorey, M.L., Evans, W.C., Kennedy, B.M., Farrar, C.D., Hainsworth, L.J., and Hausback, B., 1998, Carbon dioxide and helium emissions from a reservoir of magmatic gas beneath Mammoth Mountain, California: Journal of Geophysical Research, v. 103, no. B7, p. 15.

Stumm, W., and Morgan, J.J., 1996, Aquatic chemistry (3d ed.), New York, John Wiley and Sons, 1,022 p.

Stupfel, Maurice and LeGuern, Francois, 1989, Are there biomedical criteria to assess an acute carbon dioxide intoxication by a volcanic emission?: Journal of Volcanology and Geothermal Research, v. 39, p. 247-264.

Tuttle, M.L., Clark, M.A., Compton, H.R., Devine, J.D., Evans, W.C., Humphrey, A.M., Kling, G.W., Koenigsberg, E.J., Lockwood, J.P., and Wagner, G.N., 1987, The 21 August 1986 Lake Nyos Gas Disaster, Cameroon: U.S. Geological Survey Open-File Report 87-97, 58 p.

Table 1. Soil gas carbon dioxide volumetric concentrations, Mammoth Mountain, California

[Gas samples collected from 0.5 meter below land surface. Sample No., alphanumeric identifier on figures 2*A-G*. Latitude/longitude, coordinates in degrees-minutes-seconds; ppm, parts per million]

Sample No.	Latitude	Longitude	Carbon dioxide (ppm)	Carbon dioxide (percent)	Date
		Transect Line A			
A1	37°38'44.00"	119°02'24.33"	1,083	0.11	8/18/95
A2	37°38'44.04"	119°02'26.16"	1,628	.16	8/18/95
A3	37°38'44.58"	119°02'27.68"	22,954	2.30	8/18/95
A4	37°38'44.59"	119°02'28.52"	2,918	.29	8/18/95
A5	37°38'44.42"	119°02'29.43"	66,491	6.65	8/18/95
A6	37°38'44.77"	119°02'30.29"	262,102	26.21	8/18/95
A7	37°38'44.91"	119°02'31.08"	283,341	28.33	8/18/95
A8	37°38'45.00"	119°02'32.27"	506,241	50.62	8/18/95
A9	37°38'45.10"	119°02'33.27"	323,610	32.36	8/18/95
A10	37°38'45.91"	119°02'35.76"	37,574	3.76	8/18/95
A11	37°38'46.73"	119°02'37.37"	560,264	56.03	8/18/95
A12	37°38'47.07"	119°02'38.21"	346,864	34.69	8/18/95
A13	37°38'47.29"	119°02'39.08"	497,909	49.79	8/18/95
A14	37°38'46.27"	119°02'39.23"	304,556	30.46	8/18/95
A15	37°38'46.48"	119°02'40.69"	71,544	7.15	8/18/95
A16	37°38'46.58"	119°02'42.41"	325,727	32.57	8/18/95
A17	37°38'46.57"	119°02'43.91"	414,236	41.42	8/18/95
A18	37°38'46.34"	119°02'45.58"	433,112	43.31	8/18/95
A19	37°38'45.76"	119°02'47.16"	37,036	3.70	8/18/95
A20	37°38'46.12"	119°02'48.75"	158,160	15.82	8/18/95
A21	37°38'45.95"	119°02'50.39"	531,210	53.12	8/18/95
A22	37°38'46.17"	119°02'51.65"	493,740	49.37	8/18/95
A23	37°38'46.28"	119°02'52.32"	51,119	5.11	8/18/95
A24	37°38'46.29"	119°02'53.41"	27,576	2.76	8/18/95
A25	37°38'46.35"	119°02'54.25"	453,349	45.33	8/18/95
A26	37°38'46.53"	119°02'55.03"	21,341	2.13	8/18/95
		Transect Line B			
B1	37°38'43.20"	119°02'46.82"	3,362	0.34	8/18/95
B2	37°38'44.23"	119°02'46.08"	5,216	.52	8/18/95
B3	37°38'45.36"	119°02'45.84"	16,504	1.65	8/18/95
B4	37°38'45.53"	119°02'45.53"	46,400	4.64	8/18/95
B5	37°38'46.05"	119°02'45.51"	266,351	26.64	8/18/95
B6	37°38'47.49"	119°02'44.84"	34,026	3.40	8/18/95
B7	37°38'48.67"	119°02'44.09"	35,281	3.53	8/18/95
B8	37°38'49.72"	119°02'43.34"	32,717	3.27	8/18/95
B9	37°38'50.34"	119°02'43.08"	27,984	2.80	8/18/95
B10	37°38'51.37"	119°02'43.02"	18,189	1.82	8/18/95

Table 1. Soil gas carbon dioxide volumetric concentrations, Mammoth Mountain, California—Continued

Sample No.	Latitude	Longitude	Carbon dioxide (ppm)	Carbon dioxide (percent)	Date
		Transect Line B—Continued			
B11	37°38'51.94"	119°02'42.78"	7,011	.70	8/18/95
B12	37°38'53.08"	119°02'42.81"	830	.08	8/18/95
B13	37°38'53.26"	119°02'42.02"	2,120	.21	8/18/95
		Transect Line BP1			
BP101	37°37'00.68"	119°00'58.08"	14,627	1.46	8/2/95
BP102	37°37'00.00"	119°00'58.25"	10,040	1.00	8/2/95
BP103	37°36'58.74"	119°00'59.71"	479,717	47.97	8/2/95
BP104	37°36'58.08"	119°01'00.68"	526,371	52.64	8/2/95
BP105	37°36'57.59"	119°01'01.62"	270,271	27.03	8/2/95
BP106	37°36'56.90"	119°01'02.76"	240,009	24.00	8/2/95
BP107	37°36'55.99"	119°01'03.49"	464,482	46.45	8/2/95
BP108	37°36'55.62"	119°01'04.29"	38,802	3.88	8/2/95
BP109	37°36'55.58"	119°01'05.38"	99,614	9.96	8/2/95
BP110	37°36'55.31"	119°01'06.44"	13,071	1.31	8/2/95
BP111	37°36'54.59"	119°01'07.28"	23,184	2.32	8/2/95
BP112	37°36'53.84"	119°01'08.08"	20,306	2.03	8/2/95
BP113	37°36'53.33"	119°01'08.69"	30,960	3.10	8/2/95
BP114	37°36'52.35"	119°01'09.59"	40,014	4.00	8/2/95
BP115	37°36'51.70"	119°01'09.93"	107,468	10.75	8/2/95
BP116	37°36'50.71"	119°01'10.86"	157,552	15.76	8/2/95
		Transect Line BP2			
BP201	37°36'53.56"	119°01'00.46"	14,953	1.50	8/16/95
BP202	37°36'53.84"	119°01'02.04"	14,203	1.42	8/16/95
BP204	37°36'54.65"	119°01'05.63"	107,821	10.78	8/16/95
BP205	37°36'54.78"	119°01'06.52"	108,281	10.83	8/16/95
BP206	37°36'54.87"	119°01'07.24"	260,376	26.04	8/16/95
BP207	37°36'55.08"	119°01'08.03"	112,058	11.21	8/16/95
BP208	37°36'54.89"	119°01'08.87"	97,075	9.71	8/16/95
BP209	37°36'54.64"	119°01'09.52"	20,953	2.10	8/16/95
BP210	37°36'54.47"	119°01'10.28"	115,836	11.58	8/16/95
BP211	37°36'54.29"	119°01'11.47"	100,776	10.08	8/16/95
BP212	37°36'54.16"	119°01'12.03"	539,777	53.98	8/16/95
BP213	37°36'54.20"	119°01'13.26"	100,776	10.08	8/16/95
BP214	37°36'54.36"	119°01'14.34"	260,376	26.04	8/16/95
BP215	37°36'54.38"	119°01'15.26"	59,953	6.00	8/16/95
BP216	37°36'54.49"	119°01'16.12"	31,828	3.18	8/16/95
BP217	37°36'54.74"	119°01'16.96"	100,453	10.05	8/16/95
BP218	37°36'54.72"	119°01'17.56"	10,453	1.05	8/16/95
BP219	37°36'54.74"	119°01'18.44"	4,453	.45	8/16/95
BP220	37°36'54.82"	119°01'19.02"	1,882	.19	8/16/95
BP221	37°36'54.95"	119°01'20.07"	3,749	.37	8/16/95

Table 1. Soil gas carbon dioxide volumetric concentrations, Mammoth Mountain, California—Continued

Sample No.	Latitude	Longitude	Carbon dioxide (ppm)	Carbon dioxide (percent)	Date
		Transect Line BP2—Continued			
BP222	37°36'55.30"	119°01'20.97"	2,122	.21	8/16/95
BP223	37°36'55.87"	119°01'22.75"	2,074	.21	8/16/95
BP224	37°36'56.25"	119°01'24.12"	2,217	.22	8/16/95
BP225	37°36'56.28"	119°01'25.07"	1,834	.18	8/16/95
		Transect Line C			
C1	37°38'43.46"	119°02'40.98"	357	0.04	8/18/95
C2	37°38'44.61"	119°02'40.41"	500	.05	8/18/95
C3	37°38'45.54"	119°02'39.73"	10,847	1.08	8/18/95
C4	37°38'48.41"	119°02'39.07"	45,820	4.58	8/18/95
C5	37°38'49.76"	119°02'40.53"	830	.08	8/18/95
C6	37°38'50.05"	119°02'40.05"	1,782	.18	8/18/95
		Transect Line F			
F1	37°38'23.19"	119°02'32.41"	539	0.05	8/22/95
F2	37°38'23.60"	119°02'31.71"	506	.05	8/22/95
F3	37°38'23.92"	119°02'30.95"	493	.05	8/22/95
F4	37°38'24.30"	119°02'30.36"	573	.06	8/22/95
F5	37°38'24.57"	119°02'29.62"	610	.06	8/22/95
F6	37°38'24.90"	119°02'28.80"	515	.05	8/22/95
F7	37°38'25.24"	119°02'28.09"	1,514	.15	8/22/95
F8	37°38'25.60"	119°02'27.19"	3,848	.38	8/22/95
F9	37°38'25.95"	119°02'26.29"	3,917	.39	8/22/95
F10	37°38'26.28"	119°02'25.38"	3,279	.33	8/22/95
F11	37°38'26.68"	119°02'24.60"	3,288	.33	8/22/95
F12	37°38'26.98"	119°02'23.75"	1,438	.14	8/22/95
F13	37°38'27.80"	119°02'21.80"	1,132	.11	8/22/95
F14	37°38'28.26"	119°02'21.04"	2,270	.23	8/22/95
F15	37°38'29.01"	119°02'20.36"	1,939	.19	8/22/95
F16	37°38'29.53"	119°02'19.67"	3,402	0.34	8/22/95
		Transect Line FT			
FT1	37°36'53.50"	119°01'00.40"			
FT2	37°36'52.83"	119°00'58.37"	3,834	0.38	8/23/95
FT3	37°36'52.08"	119°00'56.42"	5,272	.53	8/23/95
FT4	37°36'51.63"	119°00'54.48"	3,404	.34	8/23/95
FT5	37°36'52.00"	119°00'51.41"	5,483	.55	8/23/95
FT6	37°36'51.86"	119°00'49.54"	5,319	.53	8/23/95
FT7	37°36'51.50"	119°00'47.01"	13,194	1.32	8/23/95
FT8	37°36'51.97"	119°00'44.55"	4,935	.49	8/23/95
FT9	37°36'55.91"	119°00'47.04"	5,843	.58	8/23/95
FT10	37°36'57.53"	119°00'46.99"	4,483	.45	8/23/95
FT11	37°37'00.52"	119°00'46.31"	12,961	1.30	8/23/95

Table 1. Soil gas carbon dioxide volumetric concentrations, Mammoth Mountain, California—Continued

Sample No.	Latitude	Longitude	Carbon dioxide (ppm)	Carbon dioxide (percent)	Date
Transect Line J					
J1	37°36'47.03"	119°01'24.03"	5,953	0.60	8/16/95
J2	37°36'46.96"	119°01'22.98"	10,453	1.05	8/16/95
J3	37°36'46.73"	119°01'22.16"	8,953	.90	8/16/95
J4	37°36'46.84"	119°01'21.32"	16,453	1.65	8/16/95
J5	37°36'46.91"	119°01'20.51"	26,953	2.70	8/16/95
J6	37°36'47.07"	119°01'19.82"	137,203	13.72	8/16/95
J7	37°36'47.08"	119°01'18.99"	198,188	19.82	8/16/95
J8	37°36'47.10"	119°01'18.11"	294,696	29.47	8/16/95
J9	37°36'47.24"	119°01'17.24"	393,201	39.32	8/16/95
J10	37°36'47.37"	119°01'16.41"	502,658	50.27	8/16/95
J11	37°36'47.40"	119°01'15.77"	577,596	57.76	8/16/95
J12	37°36'47.56"	119°01'14.95"	660,636	66.06	8/16/95
J13	37°36'48.02"	119°01'14.20"	639,576	63.96	8/16/95
J14	37°36'47.77"	119°01'12.74"	905,496	90.55	8/16/95
J15	37°36'47.76"	119°01'11.97"	703,356	70.34	8/16/95
J16	37°36'47.64"	119°01'10.29"	294,696	29.47	8/16/95
J17	37°36'47.46"	119°01'09.47"	117,114	11.71	8/16/95
J18	37°36'47.25"	119°01'07.92"	32,953	3.30	8/16/95
J19	37°36'47.76"	119°01'06.65"	51,703	5.17	8/16/95
J20	37°36'47.61"	119°01'05.32"	43,453	4.35	8/16/95
Transect Line K					
K1	37°36'37.76"	119°01'23.16"	2,217	0.22	8/17/95
K2	37°36'37.49"	119°01'21.62"	6,047	.60	8/17/95
K3	37°36'37.71"	119°01'20.67"	3,749	.37	8/17/95
K4	37°36'37.47"	119°01'19.86"	171,717	17.17	8/17/95
K5	37°36'37.43"	119°01'19.08"	266,721	26.67	8/17/95
K6	37°36'37.50"	119°01'18.27"	97,906	9.79	8/17/95
K7	37°36'37.46"	119°01'17.59"	45,209	4.52	8/17/95
K8	37°36'37.32"	119°01'16.70"	13,707	1.37	8/17/95
K9	37°36'36.96"	119°01'15.71"	9,590	.96	8/17/95
K10	37°36'36.52"	119°01'14.11"	6,047	.60	8/17/95
K11	37°36'35.81"	119°01'11.96"	46,356	4.64	8/17/95
Transect Line L					
L1	37°36'41.13"	119°01'25.03"	3,941	0.39	8/17/95
L2	37°36'41.36"	119°01'23.94"	12,941	1.29	8/17/95
L3	37°36'41.09"	119°01'22.97"	10,069	1.01	8/17/95
L4	37°36'41.33"	119°01'22.02"	11,409	1.14	8/17/95
L5	37°36'41.34"	119°01'21.11"	17,537	1.75	8/17/95

Table 1. Soil gas carbon dioxide volumetric concentrations, Mammoth Mountain, California—Continued

Sample No.	Latitude	Longitude	Carbon dioxide (ppm)	Carbon dioxide (percent)	Date
Transect Line L—Continued					
L6	37°36'41.45"	119°01'20.19"	22,899	2.29	8/17/95
L7	37°36'41.55"	119°01'19.39"	32,187	3.22	8/17/95
L8	37°36'41.47"	119°01'18.45"	49,518	4.95	8/17/95
L9	37°36'41.52"	119°01'17.58"	110,697	11.07	8/17/95
L10	37°36'41.30"	119°01'16.74"	107,021	10.70	8/17/95
L11	37°36'41.47"	119°01'15.81"	306,237	30.62	8/17/95
L12	37°36'40.96"	119°01'14.98"	203,787	20.38	8/17/95
L13	37°36'40.72"	119°01'13.88"	379,737	37.97	8/17/95
L14	37°36'40.63"	119°01'13.01"	224,359	22.44	8/17/95
L15	37°36'40.72"	119°01'11.98"	40,038	4.00	8/17/95
L16	37°36'40.64"	119°01'11.19"	10,643	1.06	8/17/95
Transect Line M					
M1	37°36'32.58"	119°01'20.28"	5,281	0.53	8/17/95
M2	37°36'33.59"	119°01'20.39"	2,983	.30	8/17/95
M3	37°36'35.35"	119°01'20.15"	6,717	.67	8/17/95
M4	37°36'36.50"	119°01'19.86"	232,701	23.27	8/17/95
M5	37°36'37.81"	119°01'19.59"	134,986	13.50	8/17/95
M6	37°36'39.27"	119°01'18.52"	56,603	5.66	8/17/95
M7	37°36'40.44"	119°01'18.20"	20,696	2.07	8/17/95
M8	37°36'41.61"	119°01'17.82"	54,017	5.40	8/17/95
M9	37°36'42.84"	119°01'17.05"	96,092	9.61	8/17/95
M10	37°36'44.03"	119°01'16.06"	220,212	22.02	8/17/95
M11	37°36'45.22"	119°01'16.02"	518,372	51.84	8/17/95
M12	37°36'46.76"	119°01'15.37"	592,467	59.25	8/17/95
M13	37°36'48.03"	119°01'14.72"	669,747	66.97	8/17/95
M14	37°36'49.06"	119°01'13.94"	595,174	59.52	8/17/95
M15	37°36'50.41"	119°01'13.77"	105,192	10.52	8/17/95
M16	37°36'51.55"	119°01'13.33"	140,687	14.07	8/17/95
M17	37°36'52.85"	119°01'13.20"	30,655	3.07	8/17/95
M18	37°36'54.07"	119°01'12.64"	342,467	34.25	8/17/95
M19	37°36'54.87"	119°01'13.17"	10,771	1.08	8/17/95
M20	37°36'55.99"	119°01'12.72"	17,537	1.75	8/17/95
M21	37°36'56.90"	119°01'12.39"	15,622	1.56	8/17/95
Transect Line O					
O1	37°39'09.03"	119°02'00.00"	22,080	2.21	8/21/95
O2	37°39'12.00"	119°01'55.00"	8,682	.87	8/21/95
O3	37°39'12.05"	119°01'49.05"	3,635	.36	8/21/95
O4	37°39'09.05"	119°01'47.00"	7,246	.72	8/21/95
O5	37°39'07.05"	119°01'40.00"	4,282	.43	8/21/95

Table 1. Soil gas carbon dioxide volumetric concentrations, Mammoth Mountain, California—Continued

Sample No.	Latitude	Longitude	Carbon dioxide (ppm)	Carbon dioxide (percent)	Date
		Transect Line O—Continued			
O6	37°39'05.00"	119°01'35.00"	5,299	.53	8/21/95
O7	37°39'01.05"	119°01'31.04"	3,572	.36	8/21/95
O8	37°38'57.35"	119°01'26.91"	9,507	.95	8/21/95
O9	37°38'50.00"	119°01'28.00"	10,948	1.09	8/21/95
O10	37°38'47.11"	119°01'28.03"	6,644	.66	8/21/95
O11	37°38'42.30"	119°01'31.72"	2,471	.25	8/21/95
O12	37°38'32.00"	119°01'28.00"	1,888	.19	8/21/95
O13	37°38'32.29"	119°01'25.88"	2,321	.23	8/21/95
O14	37°38'27.00"	119°01'23.00"	3,299	.33	8/21/95
O15	37°38'27.64"	119°01'18.94"	4,504	.45	8/21/95
O16	37°38'24.08"	119°01'17.05"	2,978	.30	8/21/95
O17	37°38'24.00"	119°01'12.00"	3,754	.38	8/21/95
O18	37°38'19.63"	119°01'16.74"	3,334	.33	8/21/95
O19	37°38'16.05"	119°01'20.00"	1,932	.19	8/21/95
		Transect Line P			
P1	37°38'58.05"	119°01'24.05"	8,448	0.84	8/22/95
P2	37°38'57.00"	119°01'18.00"	7,381	.74	8/22/95
P3	37°38'57.03"	119°01'12.00"	9,106	.91	8/22/95
P4	37°38'58.00"	119°01'03.00"	6,665	.67	8/22/95
P5	37°38'57.05"	119°00'55.05"	5,580	0.56	8/22/95
P6	37°38'55.02"	119°00'50.02"	3,080	.31	8/22/95
P7	37°38'54.07"	119°00'44.05"	6,351	.64	8/22/95
P8	37°38'54.05"	119°00'38.00"	8,170	.82	8/22/95
P9	37°38'50.00"	119°00'36.00"	5,082	.51	8/22/95
P10	37°38'48.03"	119°00'40.05"	7,019	.70	8/22/95
P11	37°38'45.07"	119°00'47.03"	4,581	.46	8/22/95
P12	37°38'41.05"	119°00'43.00"	4,260	.43	8/22/95
P13	37°38'40.00"	119°00'48.00"	2,988	.30	8/22/95
P14	37°38'39.03"	119°00'53.00"	9,659	.97	8/22/95
		Transect Line S			
S1	37°38'36.30"	119°03'02.73"	1,135	0.11	8/20/95
S2	37°38'31.65"	119°03'01.38"	1,846	.18	8/20/95
S3	37°38'27.26"	119°02'58.37"	2,430	.24	8/20/95
S4	37°38'25.79"	119°02'54.63"	2,516	.25	8/20/95
S5	37°38'19.81"	119°02'50.82"	560	.06	8/20/95
S6	37°38'13.61"	119°02'49.86"	2,370	.24	8/20/95
S7	37°38'08.86"	119°02'47.98"	3,314	.33	8/20/95
S8	37°38'06.48"	119°02'43.96"	1,103	.11	8/20/95
S9	37°38'02.40"	119°02'41.82"	627	.06	8/20/95
S10	37°37'57.90"	119°02'39.36"	800	.08	8/20/95

Table 1. Soil gas carbon dioxide volumetric concentrations, Mammoth Mountain, California—Continued

Sample No.	Latitude	Longitude	Carbon dioxide (ppm)	Carbon dioxide (percent)	Date
		Transect Line S—Continued			
S11	37°37'56.25"	119°02'35.37"	539	.05	8/20/95
S12	37°38'00.44"	119°02'34.02"	463	.05	8/20/95
S13	37°38'05.49"	119°02'33.09"	1,003	.10	8/20/95
S14	37°38'10.40"	119°02'33.45"	659	.07	8/20/95
S15	37°38'07.97"	119°02'31.04"	429	.04	8/20/95
S16	37°38'03.82"	119°02'28.50"	538	.05	8/20/95
S17	37°37'59.88"	119°02'24.49"	1,803	.18	8/20/95
S18	37°37'57.69"	119°02'19.59"	772	.08	8/20/95
S19	37°37'56.91"	119°02'13.23"	494	.05	8/20/95
S20	37°37'56.44"	119°02'07.10"	585	.06	8/20/95
S21	37°37'53.53"	119°02'02.64"	470	.05	8/20/95
S22	37°37'51.01"	119°01'59.52"	456	.05	8/20/95
S23	37°37'47.54"	119°01'54.00"	1,420	0.14	8/20/95
		Transect Line T			
T1	37°37'13.62"	119°01'39.64"	392,643	39.26	8/20/95
T2	37°37'12.80"	119°01'45.00"	72,173	7.22	8/20/95
T3	37°37'12.08"	119°01'51.12"	4,348	.43	8/20/95
T4	37°37'13.08"	119°01'59.14"	897	.09	8/20/95
T5	37°37'14.48"	119°02'06.85"	4,710	.47	8/20/95
T6	37°37'17.63"	119°02'13.72"	30,134	3.01	8/20/95
T7	37°37'22.10"	119°02'20.03"	310,372	31.04	8/20/95
T8	37°37'27.53"	119°02'23.81"	35,449	3.54	8/20/95
T9	37°37'33.10"	119°02'22.52"	28,974	2.90	8/20/95
T10	37°37'36.68"	119°02'23.02"	30,568	3.06	8/20/95
T11	37°37'39.20"	119°02'24.91"	920	.09	8/20/95
T12	37°37'40.96"	119°02'26.90"	522	.05	8/20/95
T13	37°37'43.19"	119°02'29.33"	543	.05	8/20/95
T14	37°37'45.61"	119°02'31.29"	516	.05	8/20/95
T15	37°37'48.55"	119°02'34.24"	607	.06	8/20/95
		Transect Line V			
V1	37°39'04.30"	119°02'05.00"	5143	0.51	8/21/95
V2	37°39'05.30"	119°01'57.42"	72,655	7.27	8/21/95
V3	37°39'03.50"	119°01'56.00"	13,374	1.34	8/21/95
V4	37°39'00.50"	119°01'54.50"	21,833	2.18	8/21/95
V5	37°38'56.00"	119°01'54.00"	6,361	.64	8/21/95
V6	37°38'51.56"	119°01'50.10"	8,692	.87	8/21/95
V7	37°38'47.27"	119°01'47.49"	5,763	.58	8/21/95
V8	37°38'43.00"	119°01'51.70"	4,260	.43	8/21/95
V9	37°38'40.21"	119°01'52.62"	1,151	.12	8/21/95
V10	37°38'36.50"	119°01'50.80"	1,129	.11	8/21/95

Table 1. Soil gas carbon dioxide volumetric concentrations, Mammoth Mountain, California—Continued

Sample No.	Latitude	Longitude	Carbon dioxide (ppm)	Carbon dioxide (percent)	Date
		Transect Line V—Continued			
V11	37°38'33.68"	119°01'50.29"	1,729	.17	8/21/95
V12	37°38'27.00"	119°01'53.50"	1,740	.17	8/21/95
V13	37°38'24.70"	119°02'00.01"	23,889	2.39	8/21/95
V14	37°38'27.50"	119°02'03.50"	2,459	.25	8/21/95
V15	37°38'31.96"	119°02'06.25"	3,345	.33	8/21/95
V16	37°38'35.27"	119°02'08.16"	2,806	0.28	8/21/95
		Transect Line W			
W1	37°38'32.91"	119°01'46.04"	1,510	0.15	8/21/95
W2	37°38'33.66"	119°01'40.76"	1,569	.16	8/21/95
W3	37°38'30.04"	119°01'34.00"	865	.09	8/21/95
W4	37°38'24.59"	119°01'36.80"	3,560	.36	8/21/95
W5	37°38'19.50"	119°01'37.00"	1,506	.15	8/21/95
W6	37°38'14.66"	119°01'34.66"	1,415	.14	8/21/95
W7	37°38'12.50"	119°01'30.00"	1,488	.15	8/21/95
W8	37°38'12.67"	119°01'23.13"	1,788	.18	8/21/95
		Transect Line X			
X1	37°38'34.85"	119°03'16.94"	2,380	0.24	8/19/95
X2	37°38'33.24"	119°03'15.99"	1,940	.19	8/19/95
X3	37°38'31.85"	119°03'15.52"	11,700	1.17	8/19/95
X4	37°38'30.45"	119°03'15.04"	4,040	.40	8/19/95
X5	37°38'29.00"	119°03'14.51"	21,200	2.12	8/19/95
X6	37°38'27.65"	119°03'13.99"	50,500	5.05	8/19/95
X7	37°38'26.28"	119°03'13.13"	1,420	.14	8/19/95
X8	37°38'24.77"	119°03'12.23"	969	.10	8/19/95
X9	37°38'23.32"	119°03'11.30"	11,900	1.19	8/19/95
X10	37°38'21.98"	119°03'10.48"	32,200	3.22	8/19/95
X11	37°38'20.61"	119°03'10.24"	13,200	1.32	8/19/95
X12	37°38'19.17"	119°03'09.11"	540,000	54	8/19/95
X13	37°38'18.02"	119°03'08.19"	43,500	4.35	8/19/95
X14	37°38'16.57"	119°03'07.91"	383,000	38.3	8/19/95
X15	37°38'15.14"	119°03'07.04"	107,000	10.7	8/19/95
X16	37°38'14.21"	119°03'05.91"	6,470	.65	8/19/95
X17	37°38'13.03"	119°03'04.87"	69,600	6.96	8/19/95
X18	37°38'11.95"	119°03'03.99"	19,000	1.9	8/19/95
X19	37°38'11.13"	119°03'03.02"	10,600	1.06	8/19/95
X20	37°38'10.37"	119°03'01.93"	1,630	.16	8/19/95
		Transect Line Y			
Y1	37°38'19.45"	119°03'13.61"	55,670	5.57	8/19/95
Y2	37°38'20.29"	119°03'11.58"	54,550	5.46	8/19/95
Y3	37°38'22.65"	119°03'09.19"	41,285	4.13	8/19/95
Y4	37°38'23.09"	119°03'07.92"	20,198	2.02	8/19/95
Y5	37°38'23.60"	119°03'06.91"	65,971	6.60	8/19/95

Table 1. Soil gas carbon dioxide volumetric concentrations, Mammoth Mountain, California—Continued

Sample No.	Latitude	Longitude	Carbon dioxide (ppm)	Carbon dioxide (percent)	Date
		Transect Line Z			
Z1	37°38'15.02"	119°03'18.41"	5,775	0.58	8/19/95
Z2	37°38'15.13"	119°03'16.00"	88,193	8.82	8/19/95
Z3	37°38'15.00"	119°03'13.92"	181,009	18.10	8/19/95
Z4	37°38'14.89"	119°03'12.03"	200,661	20.07	8/19/95
Z5	37°38'15.00"	119°03'10.37"	67,340	6.73	8/19/95
Z6	37°38'15.04"	119°03'09.25"	127,106	12.71	8/19/95
Z7	37°38'14.89"	119°03'07.94"	107,785	10.78	8/19/95
Z8	37°38'14.51"	119°03'06.02"	33,040	3.30	8/19/95
Z9	37°38'14.17"	119°03'04.38"	6,231	.62	8/19/95
Z10	37°38'14.42"	119°03'02.72"	16,941	1.69	8/19/95
Z11	37°38'13.91"	119°03'02.01"	201,293	20.13	8/19/95
Z12	37°38'13.99"	119°03'01.36"	25,376	2.54	8/19/95
Z13	37°38'13.71"	119°03'00.68"	13,548	1.35	8/19/95

Table 2. Carbon dioxide flux (emission rate) at selected sites, Mammoth Mountain, California, 1996

[Sample No., numeric identifier on maps; Latitude/longitude, coordinates in degrees-minutes-seconds; $(g/m^2)/d$, grams per square meter per day]

Sample No.	Latitude	Longitude	Flux $(g/m^2)/d$
	Horsehoe Lake Area—July 29-30, 1996		
1	37°36'53.29"	119°01'17.63"	53
2	37°36'50.53"	119°01'16.04"	57
3	37°36'49.28"	119°01'15.77"	2,109
4	37°36'50.58"	119°01'15.93"	726
5	37°36'48.33"	119°01'15.86"	1,306
6	37°36'47.11"	119°01'15.70"	1,276
7	37°36'45.78"	119°01'15.40"	2,306
8	37°36'44.51"	119°01'15.40"	1,059
9	37°36'43.46"	119°01'16.08"	322
10	37°36'42.36"	119°01'15.62"	198
11	37°36'41.22"	119°01'15.40"	522
12	37°36'40.07"	119°01'15.72"	113
13	37°36'38.71"	119°01'15.48"	40
14	37°36'37.95"	119°01'16.78"	14
15	37°36'36.97"	119°01'16.75"	21
16	37°36'35.74"	119°01'17.30"	19
17	37°36'35.78"	119°01'18.40"	49
18	37°36'35.78"	119°01'19.02"	301
19	37°36'36.07"	119°01'19.47"	448
20	37°36'36.29"	119°01'20.16"	93
21	37°36'36.29"	119°01'21.06"	17
22	37°36'39.13"	119°01'21.76"	20
23	37°36'39.19"	119°01'20.35"	335
24	37°36'38.79"	119°01'19.18"	359
25	37°36'38.12"	119°01'17.83"	78
26	37°36'42.85"	119°01'19.25"	39
27	37°36'42.79"	119°01'17.45"	301
28	37°36'42.84"	119°01'15.40"	179
29	37°36'42.66"	119°01'13.79"	2,190
30	37°36'42.66"	119°01'12.41"	1,563
31	37°36'45.79"	119°01'19.35"	266
32	37°36'46.27"	119°01'18.04"	395
33	37°36'46.63"	119°01'16.48"	614
34	37°36'46.70"	119°01'15.17"	1,390
35	37°36'47.20"	119°01'13.86"	375

Table 2. Carbon dioxide flux (emission rate) at selected sites, Mammoth Mountain, California, 1996—Continued

Sample No.	Latitude	Longitude	Flux (g/m^2)/d
	Horsehoe Lake Area—July 29-30, 1996—Continued		
36	37°36'47.94"	119°01'12.23"	5,640
37	37°36'49.14"	119°01'10.66"	919
38	37°36'49.49"	119°01'12.28"	209
39	37°36'47.69"	119°01'12.78"	3,313
40	37°36'54.32"	119°01'06.88"	393
41	37°36'55.54"	119°01'08.96"	788
42	37°36'55.51"	119°01'06.76"	158
43	37°36'55.56"	119°01'05.10"	170
44	37°36'56.15"	119°01'03.46"	159
45	37°36'56.79"	119°01'03.34"	2,152
46	37°36'56.79"	119°01'02.65"	904
47	37°36'57.72"	119°01'02.20"	6,651
48	37°36'57.60"	119°01'00.98"	2,257
49	37°36'57.99"	119°01'00.10"	1,227
50	37°36'57.95"	119°00'58.44"	75
	Chair 12 Area—July 31, 1996		
51	37°38'45.35"	119°02'30.85"	101
52	37°38'43.28"	119°02'31.75"	132
53	37°38'45.60"	119°02'34.55"	7
54	37°38'45.27"	119°02'33.17"	294
55	37°38'44.75"	119°02'32.21"	1,333
56	37°38'44.24"	119°02'32.15"	2,593
57	37°38'44.30"	119°02'33.24"	3,058
58	37°38'47.14"	119°02'35.81"	42
59	37°38'47.38"	119°02'37.98"	255
60	37°38'46.92"	119°02'38.83"	132
61	37°38'46.40"	119°02'39.22"	468
62	37°38'46.54"	119°02'41.50"	178
63	37°38'46.47"	119°02'42.70"	162
64	37°38'46.83"	119°02'43.14"	289
65	37°38'46.55"	119°02'45.49"	623
66	37°38'46.65"	119°02'49.52"	2,633
67	37°38'47.57"	119°02'50.61"	31
68	37°38'46.28"	119°02'51.52"	663
69	37°38'48.45"	119°02'48.75"	36
70	37°38'49.15"	119°02'44.65"	907
71	37°38'50.05"	119°02'43.18"	2,758
72	37°38'49.04"	119°02'42.85"	53
73	37°38'55.50"	119°02'43.00"	614
74	37°38'55.10"	119°02'42.50"	23
75	37°38'56.50"	119°02'43.00"	99

Table 2. Carbon dioxide flux (emission rate) at selected sites, Mammoth Mountain, California, 1996—Continued

Sample No.	Latitude	Longitude	Flux (g/m^2)/d
	Chair 12 Area—July 31, 1996—Continued		
76	37°38'56.50"	119°02'45.00"	1,367
77	37°38'55.50"	119°02'45.00"	1,590
	Reds Creek Area—September 9-12, 1996		
78	37°37'31.63"	119°02'16.23"	22,463
79	37°37'31.71"	119°02'16.23"	2,997
80	37°37'33.31"	119°02'16.81"	2,708
81	37°37'34.36"	119°02'17.37"	451
82	37°37'33.64"	119°02'19.35"	14
83	37°37'32.25"	119°02'19.02"	134
84	37°37'31.04"	119°02'18.81"	1,372
85	37°37'30.53"	119°02'20.73"	0
86	37°37'29.36"	119°02'24.00"	4,224
87	37°37'29.61"	119°02'24.10"	10
88	37°37'28.78"	119°02'23.73"	13
89	37°37'28.09"	119°02'23.36"	16
90	37°37'27.15"	119°02'22.49"	36
91	37°37'26.27"	119°02'23.80"	4,703
92	37°37'25.42"	119°02'23.54"	86
93	37°37'24.53"	119°02'23.12"	13
94	37°37'23.60"	119°02'21.58"	94
95	37°37'22.53"	119°02'20.26"	14
96	37°37'21.00"	119°02'19.16"	111
97	37°37'19.74"	119°02'17.75"	257
98	37°37'18.92"	119°02'16.91"	141
99	37°37'18.12"	119°02'16.03"	9
100	37°37'17.69"	119°02'16.71"	1,318
101	37°37'18.31"	119°02'17.75"	467
102	37°37'18.71"	119°02'19.37"	216
103	37°37'19.02"	119°02'19.07"	3,883
104	37°37'20.10"	119°02'20.10"	1,920
105	37°37'21.31"	119°02'21.37"	421
106	37°37'22.65"	119°02'22.76"	1,107
107	37°37'24.30"	119°02'23.98"	3,819
108	37°37'24.30"	119°02'24.60"	966
109	37°37'25.60"	119°02'24.69"	6,107
110	37°37'25.61"	119°02'26.56"	45
111	37°37'24.00"	119°02'26.70"	12
112	37°37'22.03"	119°02'26.45"	18

Table 2. Carbon dioxide flux (emission rate) at selected sites, Mammoth Mountain, California, 1996—Continued

Sample No.	Latitude	Longitude	Flux (g/m^2)/d
Reds Creek Area—September 9-12, 1996—Continued			
113	37°37'21.39"	119°02'24.46"	2
114	37°37'28.40"	119°02'28.77"	0
115	37°37'29.14"	119°02'27.77"	1,988
116	37°37'29.43"	119°02'28.08"	510
117	37°37'30.43"	119°02'27.10"	347
118	37°37'30.24"	119°02'27.10"	275
119	37°37'31.71"	119°02'25.35"	119
120	37°37'33.42"	119°02'23.16"	209
121	37°37'35.11"	119°02'21.58"	151
122	37°37'35.98"	119°02'21.77"	918
123	37°37'36.68"	119°02'19.59"	581
124	37°37'38.11"	119°02'18.32"	3,786
125	37°37'39.18"	119°02'17.59"	29,812
126	37°37'39.03"	119°02'17.59"	1,500
127	37°37'39.81"	119°02'17.05"	186
128	37°37'40.04"	119°02'15.92"	0
129	37°37'44.42"	119°02'09.60"	285
130	37°37'43.50"	119°02'10.49"	879
131	37°37'42.04"	119°02'12.02"	1,399
132	37°37'42.30"	119°02'12.02"	953
133	37°37'41.68"	119°02'12.34"	11
134	37°37'41.47"	119°02'13.34"	416
135	37°37'41.15"	119°02'14.30"	5
136	37°37'41.10"	119°02'14.50"	0
137	37°37'40.79"	119°02'15.21"	1
138	37°37'39.17"	119°02'17.61"	30,951
139	37°37'39.10"	119°02'17.70"	517
140	37°37'37.56"	119°02'17.20"	76
141	37°37'34.25"	119°02'15.05"	26
142	37°37'33.31"	119°02'14.63"	6
143	37°37'31.80"	119°02'13.98"	440
144	37°37'31.17"	119°02'14.74"	13
145	37°37'24.24"	119°02'24.42"	897
South Side Area—September 12, 1996			
146	37°37'14.85"	119°01'54.56"	3
147	37°37'14.60"	119°01'54.30"	1
148	37°37'14.03"	119°01'45.30"	22
149	37°37'13.88"	119°01'43.84"	54
150	37°37'13.92"	119°01'42.12"	68
151	37°37'13.99"	119°01'40.36"	231

Table 2. Carbon dioxide flux (emission rate) at selected sites, Mammoth Mountain, California, 1996—Continued

Sample No.	Latitude	Longitude	Flux (g/m^2)/d
South Side Area—September 12, 1996—Continued			
152	37°37'14.10"	119°01'39.29"	56
153	37°37'13.51"	119°01'39.04"	99
154	37°37'12.97"	119°01'40.36"	154
155	37°37'13.08"	119°01'41.73"	35
156	37°37'12.87"	119°01'43.03"	323
157	37°37'12.69"	119°01'44.55"	78
158	37°37'12.48"	119°01'45.74"	737
159	37°37'12.47"	119°01'46.10"	23
160	37°37'11.78"	119°01'45.09"	358
161	37°37'11.90"	119°01'43.61"	247
162	37°37'11.63"	119°01'42.23"	172
163	37°37'11.82"	119°01'40.67"	121
164	37°37'11.98"	119°01'39.72"	519
165	37°37'12.22"	119°01'38.83"	49
166	37°37'09.43"	119°01'38.76"	587
167	37°37'08.47"	119°01'38.25"	504
168	37°37'07.42"	119°01'39.19"	46
169	37°37'07.10"	119°01'39.99"	74
170	37°37'07.86"	119°01'36.39"	67
Mammoth Lodge Area—September 14, 1996			
171	37°39'04.00"	119°01'54.00"	24
172	37°39'04.00"	119°01'56.00"	81
173	37°39'04.00"	119°01'57.00"	49
174	37°39'04.03"	119°01'58.00"	164
175	37°39'04.05"	119°01'58.00"	273
176	37°39'05.00"	119°01'58.00"	353
177	37°39'05.03"	119°01'58.00"	179
178	37°39'05.03"	119°01'58.50"	72
179	37°39'05.03"	119°01'58.60"	3
180	37°39'06.00"	119°02'01.50"	12
181	37°39'08.00"	119°02'02.00"	7
182	37°39'07.05"	119°02'02.50"	0
183	37°39'08.00"	119°02'03.00"	17
184	37°39'01.00"	119°02'05.00"	94
185	37°39'00.00"	119°02'05.00"	43
186	37°38'59.05"	119°02'06.50"	27
187	37°38'59.05"	119°02'07.00"	32
188	37°38'59.00"	119°02'08.00"	41
189	37°39'00.00"	119°02'08.00"	57
190	37°39'00.00"	119°02'08.30"	70

Table 2. Carbon dioxide flux (emission rate) at selected sites, Mammoth Mountain, California, 1996—Continued

Sample No.	Latitude	Longitude	Flux (g/m^2)/d
Mammoth Lodge Area—September 14, 1996—Continued			
191	37°39'00.05"	119°02'08.30"	256
192	37°39'00.00"	119°02'12.00"	25
193	37°39'01.00"	119°02'12.00"	26
194	37°38'57.00"	119°02'13.00"	57
195	37°38'59.00"	119°02'13.00"	3
196	37°38'58.05"	119°02'23.00"	56
197	37°38'58.00"	119°02'23.00"	17
198	37°38'58.00"	119°02'22.00"	4
Saddle Area—September 13, 1996			
199	37°38'00.64"	119°01'56.67"	5
200	37°38'00.99"	119°01'56.19"	6
201	37°38'01.47"	119°01'55.87"	32
202	37°38'01.95"	119°01'55.64"	24
203	37°38'02.21"	119°01'55.39"	4
204	37°38'03.42"	119°01'54.87"	8
205	37°38'03.65"	119°01'54.91"	1,847
206	37°38'04.12"	119°01'55.52"	1
207	37°38'04.00"	119°01'55.50"	3
208	37°38'03.71"	119°01'56.11"	0
209	37°38'03.10"	119°01'56.09"	129
210	37°38'03.12"	119°01'54.39"	256
211	37°38'03.73"	119°01'53.80"	4,769
212	37°38'07.49"	119°02'03.85"	14
213	37°38'06.91"	119°02'08.42"	0
214	37°38'07.58"	119°02'07.53"	20
215	37°38'08.44"	119°02'06.75"	21
216	37°38'09.75"	119°02'05.30"	13
217	37°38'09.99"	119°02'05.03"	2
218	37°38'10.89"	119°02'04.51"	3
219	37°38'11.05"	119°02'03.56"	0
220	37°38'10.63"	119°02'01.96"	49
221	37°38'10.72"	119°01'59.46"	294
222	37°38'10.41"	119°01'58.64"	2
Mammoth Mountain Fumarole Area—September 13, 1996			
223	37°38'13.51"	119°01'43.24"	2,508
224	37°38'13.50"	119°01'43.00"	595
225	37°38'13.11"	119°01'43.04"	88
226	37°38'12.89"	119°01'42.71"	120
227	37°38'12.41"	119°01'42.29"	290

Table 2. Carbon dioxide flux (emission rate) at selected sites, Mammoth Mountain, California, 1996—Continued

Sample No.	Latitude	Longitude	Flux (g/m^2)/d
Mammoth Mountain Fumarole Area—September 13, 1996—Continued			
228	37°38'12.23"	119°01'42.04"	689
229	37°38'12.08"	119°01'41.60"	8
230	37°38'13.12"	119°01'41.54"	160
231	37°38'13.39"	119°01'42.16"	8,050
232	37°38'13.60"	119°01'42.00"	708
233	37°38'14.06"	119°01'42.73"	104
234	37°38'14.43"	119°01'42.95"	52
235	37°38'14.04"	119°01'43.32"	933
236	37°38'13.77"	119°01'43.60"	4,319
237	37°38'13.49"	119°01'43.85"	1,623
238	37°38'13.37"	119°01'44.30"	188
239	37°38'14.16"	119°01'44.18"	62
Dry Creek Area—September 13, 1996			
240	37°38'19.74"	119°01'15.89"	0
241	37°38'20.69"	119°01'17.06"	2
242	37°38'20.94"	119°01'13.94"	14
243	37°38'24.07"	119°01'10.13"	5
244	37°38'29.49"	119°01'25.45"	594
245	37°38'30.03"	119°01'25.13"	474
246	37°38'31.11"	119°01'28.80"	3
247	37°38'24.09"	119°01'29.31"	6
248	37°38'26.93"	119°01'22.44"	25
Red's Lake Area—August 4, 1995			
249	37°38'17.00"	119°03'00.12"	960
250	37°38'17.00"	119°03'00.10"	1,952

Table 3. Chemical analyses of water samples from Mammoth Mountain area, California

[Site, alphanumeric designation given in figure 2 and site type; Station No., U.S. Geological Survey site identifier; °C, degrees Celsius; µS/cm, microseimens per centimeter; mg/L, concentration in milligrams per liter; µg/L, concentration in micrograms per liter; —, no data]

Site	Station no.	Date	Depth of sample (m)	Altitude of land surface (meters above sea level)	Temperature water (°C)	Specific conductance, field (µS/cm)	Specific conductance, lab (µS/cm)	pH water whole field (standard units)	pH water whole lab (standard units)	[1]Alkalinity, field, as $CaCO_3$ (mg/L)
HSL Lake	373629119010801	10-20-94	14	2,745	7.0	17	22	6.7	6.9	10
		06-06-95	18	2,745	4.1	51	34	6.9	6.9	30
		06-06-95	10	2,745	3.8	31	26	6.4	6.4	10
		07-17-96	18	2,745	5.1	17	19	6.4	7.0	9
HSL-1 Monitor well	373650119011301	07-18-96	94	2,755	10.0	147	148	5.3	5.4	73
		08-18-97	94	2,755	12.0	131	136	5.3	5.5	66
LB-1 Supply well	373634119004801	10-17-95	78	2,740	6.0	158	166	7.0	7.2	82
		07-18-96	78	2,740	5.0	189	191	7.0	6.6	98
		08-19-97	78	2,740	5.5	163	170	7.1	6.9	89
CH11A Monitor well	373846119023101	07-18-96	59	2,760	4.5	163	170	5.1	5.2	80
		08-19-97	59	2,760	5.0	162	163	5.0	5.3	68
MMSA-1 Supply well	373904119021501	11-03-95	36	2,720	4.5	276	291	5.7	5.8	91
MMSA-2 Supply well	373901119012901	11-02-95	100	2,650	5.5	256	269	5.7	5.8	112
MCL Unused spring	373708119040601	07-14-94	0	2,420	8.0	265	271	5.7	5.6	128

[1]Alkalinity, field, titration to 4.5 pH.

Table 3. Chemical analyses of water samples from Mammoth Mountain area, California—Continued

Site	Station no.	Date	[2]Alkalinity, field, as $CaCO_3$ (mg/L)	[3]Alkalinity, lab, as $CaCO_3$ (mg/L)	Bicarbonate, water whole field (mg/L)	Nitrogen, ammonia, dissolved (mg/L)	Nitrogen, nitrite, dissolved (mg/L)	Nitrogen NO_2+NO_3, dissolved (mg/L)	Phosphorus ortho, dissolved (mg/L)	Calcium, dissolved (mg/L)
HSL Lake	373629119010801	10-20-94	10	11	12	0.023	0.003	<0.005	<0.001	2.2
		06-06-95	31	16	38	.419	<.001	.007	<.001	3.4
		06-06-95	11	12	12	.007	<.001	.057	<.001	2.6
		07-17-96	8	8.7	9	.013	.002	<.005	.002	1.8
HSL-1 Monitor well	373650119011301	07-18-96	70	73	89	.020	.010	.110	.040	11
		08-18-97	62	69	81	<.015	<.010	.098	.041	9.7
LB-1 Supply well	373634119004801	10-17-95	82	84	101	—	—	—	—	17
		07-18-96	98	98	120	.030	<.010	.090	.050	20
		08-19-97	90	88	109	.073	<.010	.102	.042	18
CH11A Monitor well	373846119023101	07-18-96	70	80	98	.020	.010	.170	.120	13
		08-19-97	59	80	83	<.015	<.010	.159	.113	12
MMSA-1 Supply well	373904119021501	11-03-95	94	97	115	<.015	.010	3.40	.020	15
MMSA-2 Supply well	373901119012901	11-02-95	114	122	138	<.015	<.010	2.40	.170	12
MCL Unused spring	373708119040601	07-14-94	132	134	161	<.010	<.010	<.050	.130	14

[2]Alkalinity, field, incremental titration.

[3]Alkalinity, lab, titration to 4.5 pH.

Table 3. Chemical analyses of water samples from Mammoth Mountain area, California—Continued

Site	Station no.	Date	Magnesium, dissolved (mg/L)	Sodium, dissolved (mg/L)	Potassium, dissolved (mg/L)	Chloride, dissolved (mg/L)	Sulfate, dissolved (mg/L)	Fluoride, dissolved (mg/L)	Silica, dissolved (mg/L)	Arsenic, dissolved (µg/L)
HSL Lake	373629119010801	10-20-94	0.34	1.4	0.30	0.10	0.30	0.10	4.6	<1
		06-06-95	.51	1.4	.50	.30	<.10	.20	6.5	<1
		06-06-95	.41	1.3	.40	.20	.50	.10	5.4	<1
		07-17-96	.29	1.0	.30	<.10	.40	<.10	5.2	<1
HSL-1 Monitor well	373650119011301	07-18-96	6.4	6.2	6.7	<.10	.30	.10	55	<1
		08-18-97	5.9	5.6	5.7	<.10	.30	.13	55	<1
LB-1 Supply well	373634119004801	10-17-95	4.9	7.3	4.4	.50	.80	<.10	32	<1
		07-18-96	5.8	8.5	5.3	.60	.80	<.10	33	<1
		08-19-97	5.2	7.7	4.8	.57	.67	<.10	34	<1
CH11A Monitor well	373846119023101	07-18-96	8.9	6.0	3.7	.90	2.3	.20	37	<1
		08-19-97	8.8	5.8	3.6	5.5	1.7	.22	37	<1
MMSA-1 Supply well	373904119021501	11-03-95	11	17	8.5	19	2.6	<.10	43	<1
MMSA-2 Supply well	373901119012901	11-02-95	7.3	30	3.7	4.7	2.2	<.10	50	<1
MCL Unused spring	373708119040601	07-14-94	13	15	8.6	.30	9.2	.10	65	1

Table 3. Chemical analyses of water samples from Mammoth Mountain area, California—Continued

Site	Station no.	Date	Boron, dissolved (µg/L)	Iron, dissolved (µg/L)	Manganese, dissolved (µg/L)	Lithium, dissolved (µg/L)	Solids, residue at 180°C dissolved (mg/L)	Mercury, dissolved (µg/L)	H-2/H-1 stable isotope ratio (per mil)	O-18/O-16 stable isotope ratio (per mil)
HSL Lake	373629119010801	10-20-94	<10	47	4.0	<10	6	<0.1	-96.4	-12.40
		06-06-95	<10	—	—	<10	28	<.1	—	-12.70
		06-06-95	<10	88	3.0	<10	10	<.1	—	-11.61
		07-17-96	<4.0	12	<1.0	—	13	—	—	-13.63
HSL-1 Monitor well	373650119011301	07-18-96	12	35	46	—	100	—	—	-14.04
		08-18-97	11	14	40	—	148	—	—	—
LB-1 Supply well	373634119004801	10-17-95	<10	<3.0	<1.0	<10	98	<.1	—	-14.90
		07-18-96	6.7	<3.0	<1.0	—	114	—	—	-14.65
		08-19-97	8.9	<3.0	<1.0	—	125	—	—	—
CH11A Monitor well	373846119023101	07-18-96	4.2	19	91	—	98	—	—	-14.58
		08-19-97	8.9	41	104	—	122	—	—	—
MMSA-1 Supply well	373904119021501	11-03-95	20	7.0	180	70	184	—	—	-14.86
MMSA-2 Supply well	373901119012901	11-02-95	20	5.0	6.0	150	176	—	—	-15.09
MCL Unused spring	373708119040601	07-14-94	20	5.0	3.0	50	182	<.1	—	—

Table 4. Summary of carbon dioxide flux (emission rate) measurements, Mammoth Mountain, California, summer 1996

[$(g/m^2)/d$, grams per square meter per day; Mg/d, megagrams per day; —, no data]

Location	Area of emission (hectares)	Area of tree-kill (hectares)	Number of[3] measurements	Carbon dioxide flux statistics				Standard deviation	Estimated total flux (Mg/d)
				Minimum	Maximum	Mean	Median		
Horseshoe Lake	16	12	31	39	5,640	935	395	1,188	113
Borrow Pit	2.8	1.4	11	76	6,652	1,358	788	1,920	20
Chair 12	6.8	4.6	20	53	3,058	1,001	618	1,079	48
Lodge	2.3	([1])	28	0	353	73	42	90	2
Mammoth Mtn. Fumarole	.5	([2])	17	8	8,050	1,206	290	2,092	6
Reds Creek	14.2	10.2	45	0	30,950	2,947	510	6,937	308
Reds Lake	2.3	([1])	2	960	1,952	1,506	—	—	22
Saddle	.5	([2])	24	0	4,769	313	10	1,021	2
Southside	2.2	2.2	18	3	737	217	138	209	5
Upper Dry Creek	<.1	([2])	9	.3	594	125	6	234	0
TOTALS	48	36							526

[1]Tree-kill is spotty over a large area; the boundary was not mapped.

[2]Area is above tree line of mostly devoid of trees.

[3]For Horseshoe Lake, Borrow Pit, Chair 12, and Reds Creek, only values for points inside tree kill boundaries are included. See table 2 for complete listing of all sample points and flux values.